4.4 NUCLEAR MAGNETIC RESONANCE SPECTROSCOPY OF CHLOROPHYLL

Raymond J. Abraham and A. E. Rowan

TABLE OF CONTENTS

I. INTRODUCTION

The role of NMR in the study of chlorophyll is widely recognized and appreciated. The fundamental importance of the chlorophyll function *in vivo* both as antennae and phototraps that harvest light and begin the process of photosynthesis in plants and photosynthetic bacteria is well documented.[1-3] The NMR of chlorophylls has provided vast information relevant to the biosynthetic pathways of chlorophyll formation, keto-enol tautomerism, exchangeable hydrogen sites, and much more, as well as establishing the chemical identities and structure of many previously unknown chlorophylls and their derivatives. An important advance in recent years is the understanding of chlorophyll-chlorophyll interactions which are present in the large aggregates formed *in vivo*.

The chlorophylls are members of the porphyrin family, but are characterized by an isocyclic five-membered ring attached to the γ-carbon, and carbon 6.* (The side chains are similar to those of porphyrins due to their biosynthesis.) The five-membered isocyclic ring contains a keto function at C-9 and in most chlorophylls a carbomethoxy group at C-10 which with the C-9 keto function forms a β-keto ester system which can readily enolize. The keto functions, together with the unsaturated central magnesium atom, enable chlorophylls to form coordinatively large aggregate oligomers found *in vitro*. The only remaining feature is the long phytyl aliphatic side chain formed by simple esterification of C-7 propionic acid, which confers lipid solubility and correspondingly aqueous insolubility (if no detergents are present), and hence all NMR studies have been confined to organic solvents. Figure 1 shows the structure, nomenclature, and numbering of chlorophylls, in both the Fisher and IUPAC conventions. We shall henceforth use the Fisher convention, as this has been used predominantly in previous investigations.

Because of the essential role of chlorophylls, a great deal of work has focused on their molecular structure, their interactions in solution, and their structure-function relationships. The applications of NMR in these fields have been reviewed several times,[4-6] the most recent, in 1983, by the pioneer of chlorophyll NMR, J. J. Katz.[7] Despite the structural complexity of chlorophylls, the chemical shift assignment for ^{1}H NMR is relatively easy. The protons of the macrocycle are well separated and only for protons of the vinyl group (2a and 2b), ethyl group (C-4), and the protons and side chains of ring IV are spin-spin interactions observed. The most important feature of the chlorophylls in this context is the large π-system of the macrocycle which produces an "induced ring current". This "ring current" effect causes peripheral protons in the plane of the macrocycle to be deshielded, whereas protons situated above or below the plane of the macrocycle are significantly shielded. In the case of magnesium-free derivatives, the central NH protons are strongly deshielded and appear upfield of TMS. This ring current effect accounts for the large range of chemical shift values seen for chlorophylls. In Chl **a**, the range of ^{1}H chemical shifts is about 10 ppm and in the magnesium-free derivative it is larger still, about 12 ppm.

The ring current effect was initially recognized by Abraham[8], and Becker and Bradley[9] as being extremely important in understanding chlorophyll NMR and has been reproduced by Abraham et al.,[10] using a double dipole model. This model, which successfully predicted the proton chemical shifts in methyl pyropheophorbide **a** (methyl-pyro-Pheid) **a** and its porphyrin analogue, 2-vinyl-phylloerythrin methyl ester,[10] has been applied to investigate the geometry of chlorophyll-chlorophyll dimers.[11,12] Also, the extreme sensitivity of the ring-current effects to geometry enables chlorophyll-nucleophile and chlorophyll-chlorophyll interactions to be accurately deduced and accurate geometries obtained using the double dipole method.[12] The application of this ring-current model has led to much greater understanding of the aggregate geometries present in chlorophyll species and is an important recent development in the NMR of chlorophylls.

* In contrast to the convention in other chapters of this book, the Fischer nomenclature is used throughout this chapter.

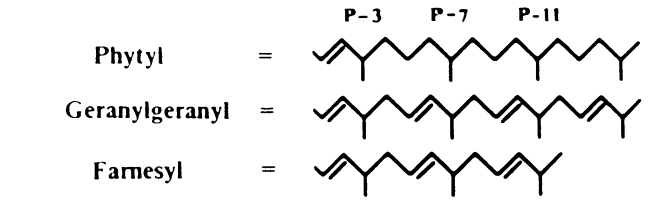

	R^1	R^2	R^3	R^4	R^5	R^{10}	R^6
Chl **a**[a]	Me	Vinyl	Me	Et	Me	CO Me	H
Chl **b**	Me	Vinyl	CHO	Et	Me	CO^2Me	H
Bchl **a**	Me	CHO	Me/H[b]	Et/H[b]	Me	CO^2Me	H
Bchl **b**	Me	Acetyl	Me/H[b]	=$CHCH_3^b$	Me	CO^2Me	H
Bchl **c**	Me	HE[c]	Me	Acetyl	Me, Et	H^2	Me
Bchl **d**	Me	HE[c]	Me	Acetyl	Me, Et	H	H
Bchl **e**	Me	HE[c]	CHO	Acetyl	Me, Et	H	Me
Bchl **g**	Me	HE[c]	Me/H[b]	=$CHCH_3^b$	Me	CO_2Me	H

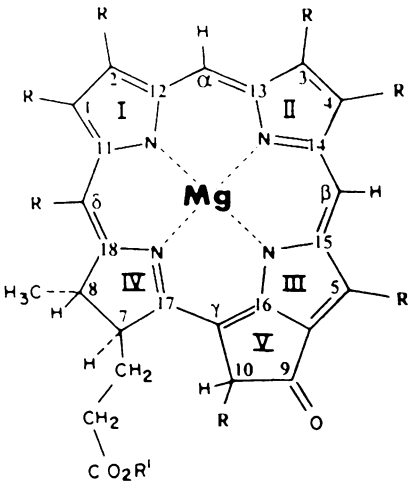

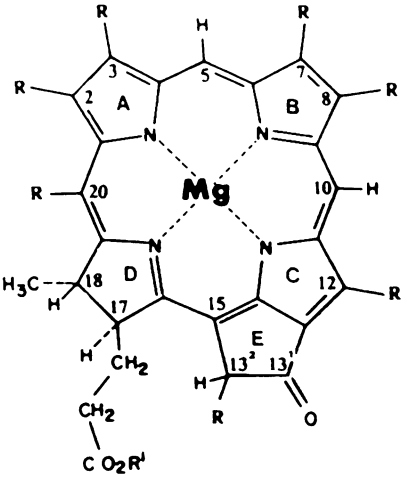

FIGURE 1. Structure and nomenclature of chlorophyll and its derivatives. (Left) Chl $\mathbf{c}_1$ and $\mathbf{c}_2$ have acrylic side chains at C_7. In Chl $\mathbf{c}_2$, there is a vinyl group at C_4; otherwise it is the same as Chl **a**. (Right) Ring II is not reduced **c**. HE = 1-hydroxyethyl.

II. ^{1}H NMR OF CHLOROPHYLL MONOMERS

Chlorophylls, when dissolved in coordinating solvents (acetone, pyridine, methanol, tetrahydrofuran, etc.) or in noncoordinating solvents in which a molar excess of these ligands has been added, give spectra characteristic of the monomer species. Thus the ^{1}H NMR chemical shifts obtained in these solutions are typical of chlorophyll-ligand and/or chlorophyll (ligand) species. The ^{1}H NMR chemical shifts, in particular those of Chl **a**, have received such extensive attention that they were described by Katz[6] as being "overdetermined". However, much of the earlier work was recorded at low field and on relatively concentrated solutions in which the ^{1}H NMR spectrum is only partially resolved and there exists the possibility of significant concentration effects. At the lower concentrations possible using modern spectrometers, the influence of adjacent macrocycles can be significantly reduced. The more resolved spectra obtained have enabled the $^3J_{HH}$ couplings to be obtained from the macrocyclic side chains, giving, in turn, valuable conformational information about these flexible parts of the chlorophyll molecule.

A. PHEOPHORBIDES

The assignment of chlorophyll was based upon the initial assignments of methyl-Pheids **a** and **b** by Closs et al.[13] In these magnesium-free chlorophylls, the large phytyl moiety is replaced by a methyl, greatly simplifying the high-field region of the spectrum allowing the assignment of the remaining aliphatic protons (4a-CH_3 and 8-CH_3). The rationale behind these assignments, which in turn applies to the magnesium-containing derivatives, has been reported in earlier reviews[4,7] and will not be repeated here. Table 1 lists the chemical shifts for several methyl pheophorbide derivatives.

The magnesium-free pheophorbides and pheophytins are significantly more concentration dependent than their chlorophyll counterparts. Table 1 shows the large chemical shift differences ($\Delta\delta$) for methyl-pyro-Pheid **a** at two different concentrations. As the concentrations increase, π-π stacking occurs[4,13] in a specific orientation and hence induces selective ring-current shifts. The ^{1}H NMR concentration dependence of methyl pheophorbides, derived from BChl **c**, with an α-hydroxyethyl group at position 2, has been investigated by Brockman et al.[18] At high concentrations (>0.1 *M*), a doubling of many of the resonances is observed (also seen for other chlorophyll derivatives with an α-hydroxyethyl), due to the formation of large aggregates. These aggregates are held together by π-π stacking and hydrogen bonding between the hydroxyl group and the C-9 keto function, which together slow the rate of the aggregate-disaggregate equilibria. This explanation has been questioned[7] since the equilibria are normally too fast to be observed by NMR, and hence the doubling is thought to be due to hindered rotation about C-2, C-2′, although this does not account for the absence of doubling in the acetylated derivatives.

The removal of the phytyl side chain and replacement with a methyl, although greatly simplifying the spectra, does not significantly affect the position of the macrocycle proton resonances. The propionic side chain in methyl-Pheid **a** has been fully analyzed by Smith et al.[19,20] At high-field strengths, the previously unresolved complex five-spin system can be fully interpreted. Decoupling of H-7 gives a complex four-spin system since all proton chemical shifts differ, due to the chiral centers at C-7, C-8, and C-10. It was found, unexpectedly, that the propionic side chain protons, 7a,7a′ and 7b,7b′, gave closely coupled multiplets which were vicinal rather than geminal pairs.

The observed couplings of the propionic side chain are reported in Table 2. Analysis of the conformation of the side chain in classical terms — anti, g^+, g^- (Figure 2) — gave, in contrast to the conformation of ethyl-Chlid **a** in the crystal[21] in which the only conformation observed is g^-, the favored conformation in methyl-Pheid **a** in solution with C-7, C-7a, C-7b, C-7c anti. The preferred conformation of the C-7,7a fragment is, however, the crystal conformation (C-7α, C-7, C-7a, C7b anti), giving the expected lateral side-chain conformation, but with an appreciable proportion with the carbomethoxy group over the chlorin ring.

The observed C-7, C-8 coupling provides information on the reduced ring IV. Calculation based on the crystal geometry of Fischer et al.,[22] in which C-7 is out of the plane of the remaining atoms of ring IV, gives a dihedral angle of 110° for H-7, H-8 consistent with the observed coupling of 2 Hz.

B. CHLOROPHYLLS

The chemical shifts of Chl **a** and several closely related derivatives are shown in Table 3. At high fields,[14,24] all the protons of the macrocycle can be positively assigned; only those of the methyl and methylene protons of the phytyl side chain (P-5 to P-15) remain undetermined, giving rise to a complex pattern at δ 1.0 to 1.2 ppm. The observed chemical shifts of Smith et al. are in general downfield by about 0.1 to 0.2 ppm from those observed by Katz et al.,[6] attributable to general anisotropic shifts from the Chl ring current at the higher concentrations used in Reference 6. The assignment of H-8 and H-7 is reversed from those

TABLE 1
^{1}H Chemical Shift of Methyl Pheophorbides and Pheophytin[a]

Proton	Phe a[b] (0.005 *M*)	Methyl Pheid a[c] (0.06 *M*)	Methyl pyro-Pheid a (0.06 *M*)[c]	(0.007 *M*)[d]	Methyl Pheid b[c] (0.08 *M*)	Methyl BPheid a[c] (0.05 *M*)	Methyl BPheid c[f] (0.05 *M*)	Methyl BPheid d[e] (0.014 *M*)
α	9.38	9.15	9.20	9.40	9.76	8.96	9.44	9.60
β	9.52	9.32	9.32	9.52	8.89	8.47	9.49	9.49
δ	8.55	8.50	8.50	8.56	8.47	9.40	—	8.48
2a	8.00	7.85	7.98	8.02	7.75	—	7.90	6.35
2b	6.28/6.18	6.12/6.02	6.25/6.15	6.29/6.18	6.16/6.08	3.15[g]	6.22/6.09	2.10
10	6.26	6.22	5.13	5.27/5.11	6.22	6.08[h]	5.23	5.23/5.09
8	4.46	4.40	4.42	4.49	4.45	4.28[i]	4.27	4.44
7	4.41	4.13	4.23	4.30	4.15	4.02	n.r.	4.24
δ-CH_3	—	—	—	—	—	—	3.86	—
10b	3.88	3.88	—	—	3.95	3.84	—	—
5a	3.68	3.62	3.58	3.68	3.46	3.48	1.96[j]	4.06
7d	—	3.57	3.58	3.61	3.62	3.57	3.60	3.62
4a	3.68	3.48	3.50	3.70	3.37	2.20	1.67	3.67
1a	3.40	3.32	3.35	3.41	3.28	3.44	3.48	3.37
3a	3.23	3.15	3.13	3.25	10.58	1.72	—	3.22
7a	2.63	—	—	2.70	—	—	—	
7a′	2.34	—	—	2.31	—	—	—	2.20—2.67
7b	2.49	—	—	2.56	—	—	—	
7b′	2.19	—	—	2.29	—	—	—	
8a	1.80	1.82	1.72	1.81	1.88	1.79	1.48	1.77
4a	1.69	1.60	1.55	1.70	1.48	1.10	1.67	3.67
NH	−1.6/−1.8	−1.75	−1.85	0.48/−1.67	0.83/−2.15	0.46/−0.96	—	0.34/−1.78

[a] All shifts referenced to TMS in deuteriochloroform.
[b] Reference 14.
[c] Reference 7.
[d] Reference 15.
[e] Reference 16.
[f] Reference 17. A mixture with position 4 occupied by ethyl, *n*-propyl, and *i*-butyl and position 5 occupied by methyl and ethyl.
[g] The methyl group of the acetyl group at position 2.
[h] Includes proton at position 3.
[i] Includes proton at position 4.
[j] An ethyl group at position 5.

TABLE 2
Observed Proton Coupling Constants (Hz)

	Methyl Pheid a[a]	Phe a[b]	Chl a[c]	Chl a[d]	BChl a[e]
7a, 7a′	−14.0	−14.2	−14.1	−14.7	−14.0
7a, 7b	6.7	6.5	6.4	7.4	6.4
7a, 7b′	9.9	9.7	9.8	8.3	9.9
7a′, 7b	9.3	9.5	9.7	8.5	9.7
7a′, 7b′	5.2	5.0	5.0	6.3	5.2
7b, 7b′	−15.7	−15.5	−15.9	−15.7	−15.8
7, 7a	3.2	3.1	3.7	—	3.7
7, 7a′	9.0	8.5	8.6	—	8.7
7, 7b	−0.2	—	−0.2	—	−0.2
7, 7b′	−0.2	—	0.0	—	0.0
7, 8	1.6	2.0	1.8	1.8	2.0
8, 8a	—	—	7.3	—	7.2
P-1, P-2	—	6.6	7.0	6.5 (7.1)	7.0
P-1′, P-2	—	7.5	7.0	8.0 (7.3)	7.0
P-1′, P-1	—	−12.4	—	−13.3 (−12.4)	—

[a] Reference 19, in $CDCl_3$ solution.
[b] Reference 14, in $CDCl_3$ solution.
[c] Reference 23, in tetrahydrofuran-d_8 solution.
[d] Reference 14, in $CDCl_3$-methanol-d_4 solution and in acetone (parentheses).
[e] Reference 23, in tetrahydrofuran-d_8 solution.

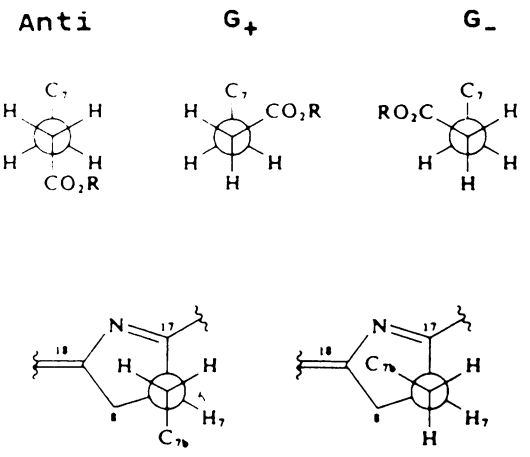

FIGURE 2. Rotamer conformation and geometry of the propionic side chain.

given previously. At the higher applied fields, the H-7, H-8 resonances are well separated and can be unequivocally assigned. The chemical shifts of Chls are not as concentration dependent as their magnesium-free counterparts, but are very strongly solvent dependent,[14] this solvent effect being associated with the coordination state of the central Mg atom. Electronic absorption spectra measured for Chl **a** indicate that the Mg atom is predominantly hexacoordinated in tetrahydrofuran and pentacoordinated in acetone.[7]

In addition to Chl **a** and Chl **b**, there are two other chlorophylls, Chl $\mathbf{c}_1$ and Chl $\mathbf{c}_2$[25] (Chl $\mathbf{c}_3$ has been characterized recently; see Chapter 1.1), both being similar to each other and closely related to Chl **a**. These chlorophylls are common pigments in various marine algae (see Chapter 1.1). They are porphyrins, not chlorins, but both have ring V present

TABLE 3
^{1}H NMR Chemical Shifts of Monomeric Chlorophylls

	Chl a[a] (0.003 *M*)	Phy a[b] (0.005 *M*)	Pyro-Chl a[c]	Methyl pyro-Chl a$_d$ (0.004 *M*)	Chl b[e]	Chl c$_1$[f]	Chl c$_2$[f]
α	9.29	9.38	9.22	9.29	9.87	9.95	10.10
β	9.54	9.52	9.46	9.55	9.55	9.90	10.00
δ	8.32	8.55	8.37	8.30	8.18	9.80	9.92
3-CHO	—	—	—	—	10.92	—	—
2a$_{trans}$	7.98	8.00	7.99	8.00	7.85	8.28	8.33
2b$_{cis}$	6.19	6.28	5.99	6.19	5.98	6.34	6.35
2c	6.01	6.18	—	6.00	6.15	6.04	6.06
10H	6.24	6.26	4.33	5.07/4.96	6.10	6.72	6.84
8H	4.40	4.46	4.09	4.39	4.45	—	—
7H	4.08	4.21	4.21	4.17	4.15	—	—
4a	3.75	3.68	—	3.75	—	—	8.33
10b	3.99	3.88	—	—	3.95	(3.5—4.0)	(3.5—4.0)
5a	3.64	3.68	3.22	3.56	3.52	(3.5—4.0)	(3.5—4.0)
1a	3.30	3.40	3.22	3.33	3.22	(3.5—4.0)	(3.5—4.0)
3a	3.27	3.23	3.16	3.25	—	(3.5—4.0)	(3.5—4.0)
7a	2.53	2.63	2.09	2.52	2.35	—	—
7a′	2.41	2.34		2.38		—	—
7b	2.38	2.49	2.40	2.26	2.35	—	—
7b′	2.08	2.19		1.98		—	—
8a	1.78	1.80	1.64	1.70	—	(3.5—4.0)	(3.5—4.0)
4b	1.71	1.69	1.58	1.70	—	1.67	6.32/6.04
P-1	4.26	4.50/4.43	4.38	—			
P-2	5.07	5.13	4.97	—			
P-3a	1.52	1.56	1.45	[7d—3.62]			
P-4	1.86	1.90	1.75	—			
P-5	1.0—1.2	1.0—1.3	1.17, 1.12	—			
P-15				—			
P-7a				—			
P-11a	0.85	0.85	0.77, 0.74	—			
P-15a	0.81, 0.79	0.80, 0.78	0.70, 0.67	—			
P-16				—			

[a] Reference 14, in $CDCl_3$ solution with 5 μl methanol d_4, referenced to $CHCl_3$ at 7.261 ppm.
[b] Reference 14, in $CDCl_3$ solution, referenced to TMS.
[c] Reference 7, in acetone-d_6.
[d] Reference 22, in $CDCl_3$ and 30 μl pyridine-d_5.
[e] Reference 7, in $CDCl_3$/CD_3OD solution.
[f] Reference 23, in tetrahydrofuran-d_8 and in TFA (parentheses).

(Figure 1). Unlike all other chlorophylls, they do not possess an esterifying alcohol at position 7 and hence are free acids. With the removal of resonances due to an esterifying alcohol, and all those of the reduced pyrroline rings, the spectra are very simple. Apart from the CH_3 singlets, Chl **c**$_2$ shows no resonances high field of δ 6 ppm, and Chl **c**$_1$ likewise, except for ethyl proton resonances in this region. The C-7 side chain is characterized by an AX pattern due to the transacrylic acid proton. Quantitative estimates of the ratio of Chl **c**$_1$ to Chl **c**$_2$ in a mixture can be accurately and simply obtained by simple integration of the respective methine protons.

Almost all chlorophylls are esterified in the 7-propionic acid side chain with a long aliphatic alcohol. Although in Chl **a** and Chl **b** they are only esterified by phytol, this is not the case for the bacteria chlorophylls (BChl), where the most common alcohols other than phytol are geranyl-geraniol BChl **a**,[26] BChl **c**,[27] and BChl **g**,[28] farnesol BChl **a**,[29] BChl **c**,[30] BChl **d**,[31] and BChl **e**,[27] and stearol BChl **c**[27] (Figure 1). The farnesol esterifying alcohol

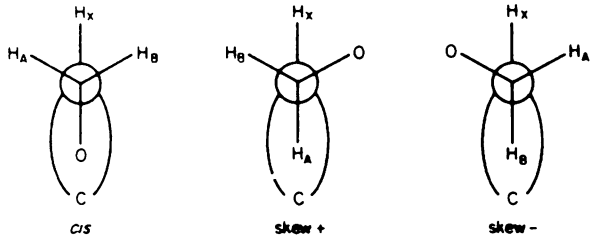

FIGURE 3. Rotamers about the P-1/P-2 ($OCH_2CH{=}C$) fragment of the phytyl side chain.

is characterized by the olefinic CH_3 singlets at $\delta \sim 1.6$ ppm and the 1-methylene doublet at 3.96 ppm. The geranylgeraniol function with four double bonds produces additional olefinic resonances in the region δ 4 to 5 ppm. In addition to these resonances, all the resonances of the esterifying alcohol show a general deshielding compared to phytol.

The observed couplings in the C-7 side chain of pheophytin (Phe) **a**[14] (Table 2) were found to be identical, within experimental error, to those of the methyl pheophorbide, suggesting identical conformations and confirming that replacement of the phytyl with methyl does not affect the macrocycle. A similar analysis of the C-7 side chain for Chl **a** by Smith et al.[14] found that the side-chain conformation differs significantly from that of the magnesium-free chlorin. Inspection of the couplings for Chl **a** showed that they tend to be more equal than in Phe **a**, implying a more equal rotamer distribution than in methyl-Pheid **a**. This conformational difference was confirmed by the chemical shifts, where δ 7a′ > δ 7b in Chl **a**, but the reverse is observed in methyl-Pheid **a** and Phe **a**. Analysis of the Chl **a** phytyl chain in an alternative solvent (THF)[24] yielded couplings identical to those of the magnesium-free derivatives. The couplings, although obtained at 60°C, in order to shift the water resonance downfield, are significantly different in the different solvents (Table 2). This solvent effect can be simply accounted for by the coordination at the central Mg. In the hexacoordinated THF solution, the Mg is in the plane of the macrocycle, whereas in the pentacoordinated acetone solution, the Mg is out of the plane by about 0.4 Å.[21] This lack of planarity in the pentacoordinated species can, in turn, especially affect ring IV and V, resulting in conformational change in the C-7 side chain. Alternatively, the preference for a larger proportion of rotamer over the chlorin ring in the pentacoordinated species could be accounted for by a weak Mg-to-carbonyl bond (C-7c), probably via a water molecule, which cannot occur in the hexacoordinated species or the magnesium-free derivatives.

The conformer preferences of the P-1,2 fragment were determined similarly from the couplings. By comparison with conformer preferences observed for allyl methyl ether[32] where J_g and J_t for the $=CHCH_2O$ fragment are 2.8 and 11.5 Hz, respectively, the conformation of the phytyl side chain was predicted. In both Chl **a** and Phe **a**, there was no evidence for the *cis* conformer (Figure 3), although this is populated in the allyl methyl ether. The two skew conformations were found to be equally populated in all spectra analyzed.

C. BACTERIOCHLOROPHYLLS

Bacteriochlorophylls are an important part of the chlorophyll family. The central magnesium in BChls, as in all chlorophylls, is removed by the common acid-catalyzed *trans*-esterification of the aliphatic alcohol by methanol and ethanol. This standard procedure, as well as simplifying the NMR, simplifies the mass spectroscopy and aids in the separation by chromatography. As a consequence of this practice, most ^1H NMR data are only available for the pheophorbide derivatives. Table 4 lists the proton chemical shifts for bacteriochlorophylls and bacteriopheophorbides.

BChl **a** from *Rhodopseudomonas (Rp.)* strains contains the phytol as the esterifying alcohol. In contrast, BChl **a** from *Rhodospirillum (Rs.) rubrum* contains geranylgeraniol. BChl **a** is thought to form a dimer in the photosynthetic reaction center and to be the primary electron donor of photosynthesis. As a consequence, the spectra of BChl **a** has been reexamined at high field.[24,33] The observed chemical shifts are in agreement with previous values measured in acetone, but differ markedly from those recorded in pyridine-d_5 solution.[7] The observed couplings of the propionic side chain were found to be identical to Chl **a** in the same solvent (Table 2). The application of the coupling constant analysis to the conformations in the 4-4a fragment of BChl **a** gives rotamer populations of about 0.6, 0.3, and 0.1. The population of H4-C4-4a-4b anti conformer (the 4b methyl group over ring 2) is 0.3. Steric constraints suggest that the most populated rotamer is 3-4-4a-4b anti. Comparison of the H3-H4 coupling to that of H7-H8, 2.8 Hz and 2.0 Hz, respectively, indicates a larger dihedral in ring II, which in turn implies that IV is more buckled than ring II.

It must be noted that the vicinal couplings are not solely dependent upon the dihedral angle, but also on the bond angles and bond lengths. This dependence is difficult to determine and hence can lead to error in the calculated rotamer population. It is possible, however, to follow relative trends in rotamer population for different chlorophylls through vicinal couplings. The similarity between the Chl **a** and BChl **a** couplings indicates the structural similarities which are a result of analogous delocalization pathways, where the C-3=C-4 double bond in Chl **a** is to some extent isolated from the conjugated system. Evidence for this comes from the acid, base properties of pyropheophytin (see ^{13}C NMR).

BChl **b** differs from BChl **a** by the replacement of the 4-ethyl group by a vinylic side chain. It is commonly found in *Rp. viridis* and a few other photosynthetic bacteria and is responsible for the extremely long absorption wavelength in these species. The only difference between the ^1H NMR spectra[34] and that of BChl **a** is due to the vinyl group. The coupling between the 3 and 4a protons gives rise to a doublet of doublets (J = 2 Hz, J = 7 Hz) at low field (δ = 6.84 ppm), the small coupling being J(3,4a) and the large coupling, J(4a,Me). As a further consequence of the C-4 vinyl group, the β-proton resonance is shifted to a lower field, while all other resonances are essentially identical to those of BChl **a**.

BChls **c**,[35] **a**,[36] and **e**[27] all lack the 10-carbomethoxy group and can be regarded as pyrochlorophylls. These BChls are found in green and brown photosynthetic bacteria and are sometimes referred to as "chlorobium chlorophylls". They are unusual when compared to natural chlorophylls in that they are a mixture of various homologues, bearing various alkyl side chains at the C-4 and C-5 position. BChls **c** and **d** have either ethyl or methyl groups at the C-5 position, while BChl **e** bears only an ethyl substituent at that position. Also, BChls **c** and **e** contain a novel methyl group at the δ *meso* position. BChls **c**, **d**, and **e** have a characteristic 2-(α-hydroxyethyl) substituent. A 2-(1-hydroxyethyl) derivative of Chl **a** has been recently isolated from a mutant of BChl **a**-producing bacterium *Rp. sphaeroides* and is suggested as an intermediate in the conversion of the 2-vinyl group of Chl **a** to the 2-acetyl group of BChl **a**.[37] This substituent shows up on the ^1H NMR spectra as a low-field quartet at δ 6.1 to 6.6 (J = 6.9 Hz for BChl **d**), and a high-field doublet at about δ 2.0. Due to the lack of a 10-carbomethoxy derivative, a characteristic AB quartet is observed at about δ 5.0 to 6.0. BChl **e**, isolated from *Chlorobium phaeovibrioides*, has the same relationship to BChl **c** as does Chl **b** to Chl **a**. The spectral features are very similar, with only two low-field methine resonances, and the presence of the C-3 CHO affects the α-*meso* proton chemical shift.

A bacteriochlorophyll derived more recently from *Heliobacterium chlorum* is BChl **g**.[27] It is structurally very similar to BChl **b**, with vinylic groups at C-2 and C-4 and a 10-carbomethoxy ester. The esterifying alcohol was geranylgeraniol, showing a large multiplet at 1.94 to 1.98 (CH_2) and a large multiplet at 5.0 to 5.1 ppm corresponding to the four olefinic hydrogens. Table 4 shows the observed chemical shifts for the magnesium BPheid **g**.

TABLE 4
^{1}H Chemical Shift of BChls a, b, d and BPheids c, e, and g (Ref. TMS)

Assignment	BChl a[a] (0.02 *M*)	BChl b[b] (0.06 *M*)	Me BPheid-c[c] (0.04 *M*)	BChl d[d] (0.005 *M*)	Me BPheid-e[e] (0.05 *M*)	BPheid-g[f]
α	9.00	9.41	9.90	9.38	10.58	8.22
β	8.46	8.93	9.41	9.49	9.42	8.60
δ	8.36	8.39	—	8.19	—	8.06
10	6.01	6.43	5.17	5.16, 5.02	5.20	5.96
3	4.33	4.93	—	—	—	~5.00
4	4.09	—	—	—	—	—
7	4.01	4.10	4.14	4.19	—	4.15
8	4.35	4.21	4.55	4.38	4.58	~4.45
2a	—	—	6.47	6.21	6.56	7.71
4a	2.37/2.12	6.84	3.68	3.71	1.72	6.94
1a	3.46	3.34	3.48	3.23	3.53	3.19
2b	3.03	2.99	2.12	2.06	2.15	6.11/6.06
3a	—	1.66	3.26	3.22	11.07	~5.0
4b	1.15	2.01	1.68	1.67	1.20	2.27
5a	3.38	3.45	3.61	4.01	4.01	3.38
8a	1.68	1.41	1.41	1.72	1.51	1.81
10b	3.71	3.66	—	—	—	3.83
δ-CH_3	—	—	3.85	—	3.86	—
7a	2.53	≈2.5	—		—	
7a′	2.33		—		—	
7b	2.42	≈2.5	—	2.2—2.6	—	2.0—2.7
7b′	2.13		—		—	
P-1	4.51			4.35		
P-2	5.24		[3.58][g]	5.16	[3.62][g]	
P-3a	1.63			1.61		
P-4	1.95			1.9—2.05		
P-5	(1.43)					
P-15	(1.04)					
P-15a	0.88					
P-7a	0.86			1.57		
P-11a	0.84			1.53/1.50		

[a] Reference 33, at 60°C in THF.
[b] Reference 34, in pyridine-d_5.
[c] Reference 35, in $CDCl_3$. Methyls at positions 3 and 5 and an ethyl at position 4.
[d] Reference 23, in $CDCl_3$ plus 20 μl of CD_3OD. Esterifying alcohol is farnesol.
[e] Reference 27, in $CDCl_3$, with a mixture of alkyl groups at position 4.
[f] Reference 28, in $CDCl_3$.
[g] 7d Methyl.

D. CHLOROPHYLL RELAXATION TIMES

The spin lattice relaxation times (T_1), n.O.e enhancements, and long-range coupling constants for chlorophylls have been obtained by Sanders et al.[38,39] The assignments obtained by Sanders, made on the basis of the T_1, n.O.e, and long-range couplings, are in agreement with assignments previously made. The T_1 values observed for the methyl protons are mainly due to steric crowding and distance from the macrocycle; hence, long values are observed for the 10b and 7d methyls. The T_1 of the methine protons are, however, dependent upon the substitution pattern of the macrocycle. The magnesium-free derivatives, as a general rule, have considerably longer relaxation times than their magnesium-containing counterparts. The application of this method to spectral and structural assignments is difficult to judge, since T_1 error limits are not certain and the observed differences in T_1 are relatively small.

TABLE 5
Comparison of the ^{1}H NMR Chemical Shifts (60 MHz, δ [ppm] from Internal TMS) of 10(*R*)- and 10(*S*)-Chlorophylls in Acetone-d_6, $c \simeq 2 \times 10^{-2}$ mol/l

	$\delta_{Chl\ a}$ ($\delta_{Chl\ b}$)	$\delta_{Chl\ a'}$ ($\delta_{Chl\ b'}$)	Δδ	Multiplicity
H-β	9.69 (10.09)	9.67 (10.07)	0.02 (0.02)	s
H-α	9.37 (9.84)	9.35 (9.80)	0.02 (0.04)	s
H-δ	8.53 (8.44)	8.48 (8.39)	0.05 (0.05)	s
H-10	6.15 (6.13)	6.06 (6.03)	0.09 (0.10)	s
P-H-2	5.01 (5.05)	5.19 (5.22)	−0.18 (−0.17)	t,J = 7 Hz
P-1-CH_2	4.28 (4.30)	4.45 (4.47)	−0.17 (−0.17)	d,J = 7 Hz
10b-CH_3	3.81 (3.83)	3.76 (3.77)	0.05 (0.06)	s
5a-CH_3	3.58 (3.57)	3.56 (3.53)	0.02 (0.04)	s
1a-CH_3	3.32 (3.27)	3.31 (3.26)	0.01 (0.01)	s
3a-CH_3(–CHO)	3.27 (11.19)	3.26 (11.19)	0.01 (0.00)	s
7a-CH_2	~2.51 (~2.51)	~2.30 (~2.34)	~0.21 (~0.17)	m
7b-CH_2	~2.29 (~2.35)	~2.19 (~2.24)	~0.10 (~0.11)	m
8a-CH_3	1.75 (1.76)	1.58 (1.59)	0.17 (0.17)	d,J = 7 Hz
P-3a-CH_3	1.52 (1.53)	1.60 (1.61)	−0.08 (−0.08)	s

From Hynninen, P. H. and Lötjönen, S., *Magn. Reson. Chem.*, 23, 605, 1985. Copyright 1985 by John Wiley & Sons, Ltd. Reprinted by permission.

E. CHLOROPHYLL EPIMERS

The epimers of Chl **a** and **b** were discovered by Strain et al.,[40] as small, fast-running satellite bands in the course of column chromatography on a sucrose column, and are diastereomers epimeric at position C-10. Confirmation of this is given by the similar chemical shifts of the two diastereotopic C-10 protons of Chl **a** and Chl **a′** with those of the two nonequivalent C-10 protons of pyro-Chl **a**. A suggestion that Chl **a′** was in fact the enol[41] form of Chl **a** was disproved by the observation of the interconversion between **a** and **a′** at low temperature by ^{1}H NMR.[42] The application of ^{1}H NMR spectroscopy, in order to reveal the conformational differences between the C-10 epimeric chlorophyll, was restricted by the uncertainty of the high-field assignments due to impurities. Improved methods developed recently[43] in the preparations of these species has allowed a more complete assignment of their ^{1}H NMR spectra and a more detailed analysis of the conformational differences between the C-10 epimeric chlorophyll derivatives.[44] Table 5 shows the chemical shift differences between Chl **a** and Chl **a′** and Chl **b** and Chl **b′**.

Using a highly purified Chl **a′** sample, the enolization-epimerization equilibrium was much slower in acetone than previous investigations had found.[42] The interconversion could be observed at room temperature. This considerably reduced rate was attributed to the purer Chl **a′** having less trace amounts of Lewis base or acid, which accelerate the enolization. (Analysis of this epimerization by Watanabe et al.,[44a] using high-resolution HPLC, found that the rate for Chl **a′** to Chl **a** is even slower than that observed by Hynninen and Lötjönen,[44] using NMR. They suggest that the Chl **a** sample used must still have contained trace amounts of potential base.) Examination of the Δδ for Chl **a′** to Chl **a** revealed strong steric constraints of the C-7 side chain in Chl **a′**. The P-2 H triplet and the P-1 CH_3 doublet move upfield, while the 7a and 7b CH_2 multiplets move in the opposite direction. Even more surprising is the large shielding effect at P-3a CH_3. The flexibility of ring IV is confirmed by the large Δδ seen for 8a-CH_3. The Δδs observed for Chl **b** closely approximate those of Chl **a** except for a slight difference in the α-methine and 5a methyl, which can be attributed to the anisotropic effect of the formyl group.

A comparison of the observed Δδ (10[*R*] vs. 10[*S*]) for Pheo **a** and **b** is shown in Table 6. The observed rate of interconversion of *R* to *S* is considerably slower than in the mag-

TABLE 6
Comparison of the ^1H NMR Chemical Shifts (60 MHz, δ [ppm] from Internal TMS) of 10(*R*)- and 10(*S*)-Pheophytins in Acetone-d_6 ($c \approx 2 \times 10^{-2}$ mol/l)[a]

	$\delta_{Phe\ a}$ ($\delta_{Phe\ b}$)	$\delta_{Phe\ a'}$ ($\delta_{Phe\ b'}$)	Δδ	Multiplicity
H-β	9.47 (9.40)	9.41 (9.45)	0.06 (−0.05)	s
H-α	9.13 (9.01)	9.07 (9.07)	0.06 (−0.06)	s
H-δ	8.79 (8.73)	8.78 (8.73)	0.01 (0.00)	s
H-2a(X)	7.94 (7.68)	7.91 (7.64)	0.03 (0.04)	dd, J(AX) = 12 Hz J(BX) = 18 Hz
H-2b(B)	6.20 (6.19)	6.17 (6.16)	0.03 (0.03)	dd, J(AB) = 2 Hz J(BX) = 18 Hz
H-2b(A)	6.07 (6.08)	6.04 (6.05)	0.03 (0.03)	dd, J(AB) = 2 Hz J(AX) = 12 Hz
H-10	6.32 (6.33)	6.24 (6.26)	0.08 (0.07)	s
P-H-2	4.99 (5.09)	5.24 (5.27)	−0.25 (−0.18)	t, J = 7 Hz
P-1-CH_2	4.31 (4.44)	4.53 (4.56)	−0.22 (−0.12)	d, J = 7 Hz
10b-CH_3	3.88 (3.96)	3.83 (3.89)	0.05 (0.07)	s
5a-CH_3	3.58 (3.45)	3.53 (3.31)	0.05 (0.14)	s
1a-CH_3	3.34 (3.28)	3.33 (3.26)	0.01 (0.02)	s
3a-CH_3(–CHO)	2.95 (10.42)	2.90 (10.45)	0.05 (−0.03)	s
7a-CH_2	~2.48 (~2.58)	~2.41 (~2.50)	~0.07 (~0.08)	m
7b-CH_2	~2.41 (~2.44)	~2.33 (~2.35)	~0.08 (~0.09)	m
8a-CH_3	1.83 (1.93)	1.66 (1.73)	0.17 (0.20)	d, J = 7 Hz
P-3a-CH_3	1.50 (1.55)	1.60 (1.63)	−0.10 (−0.08)	s
NH_I	0.31 (−0.51)	(0.44) (n.r.)	−0.13 (n.r.)	s
NH_{III}	−1.92 (−2.56)	−1.67 (−2.18)	−0.25 (−0.38)	s

[a] The δ values of the methine bridge protons depend sensitively on concentration, owing to π-π interaction between the macrocycles; to prevent the interaction, 20 μl of pyridine-d_6 were added to the solution.

From Hynninen, P. H. and Lötjönen, S., *Magn. Reson. Chem.*, 23, 605, 1985. Copyright 1985 by John Wiley & Sons, Ltd. Reprinted by permission.

nesium-containing chlorophylls. In chloroform at room temperature, Ellsworth and Storm[45] found that methyl-Pheid **a**′ appears to be stable indefinitely. In order to enhance the rate, 20 μl of pyridine were added and the temperature was elevated to 50°C. Pyridine has the additional advantage of preventing the π-π interactions common in the pheophorbides. The Δδ observed for the pheophytins are of the same order of magnitude as those of the epimeric chlorophylls. The large effect observed for the N-H protons can be used as a basis for assignment. The high-field resonance has a larger Δδ and must be the N-H protons of ring III due to its closer proximity to C-10. Although pyridine was added, π-π stacking still occurred in Chl **b**, as indicated by the observed upfield shifts for α and β methine protons. This extra π-π stacking in the Chl **b** case could be due to additional intermacrocyclic bonding between the C-3 aldehyde and the C-9 keto functions (see Chapters 1.8 and 1.9).

The measured equilibrium for Chl **a** and its equivalent magnesium-free pheophytin (Table 7) reveal that the 10(*R*) form of Chl **a** is significantly favored in both cases. (The calculated Gibbs free energy for the epimerization of Chl **a**′ to Chl **a** by Watanabe et al. was −2.8 ± 0.1 KJ/mol.) The observed thermodynamic results appear contradictory to the observed chemical shifts as the larger Δδ observed for the pheophytin equilibria suggest more pronounced conformational alterations of Pheid **a**′ (10[*S*] form), which in turn stabilizes this form with respect to Pheid **a**, yet in the pheophytin case, the 10(R) form is more favored in the magnesium-free derivative. This suggests that additional factors determine the stability of the macrocycle. Similar equilibrium constants were obtained for the Chl **b** and Pheid **b**

TABLE 7
Determination of the Equilibrium Constant (K) and Free-Energy Change (ΔG°) for the Equilibria of the C-10 Epimeric Chlorophylls and Pheophytins in Acetone Solution[a]

Reaction	10(*R*) form (%)	10(*S*) form (%)	K	ΔG° = −RT in K (J/mol)
10(*S*)-Chl **a** ⇄ 10(*R*)-Chl **a**	80	20	4.00	−3440
10(*S*)-Pheo **a** ⇄ 10(*R*)-Phe **a**	88	12	7.33	−4950

[a] Total Chl or Phe concentration ≈2 × 10^{-2} mol/l; temperature = 298 K.

From Hynninen, P. H. and Lötjönen, S., *Magn. Reson. Chem.*, 23, 605, 1985. Copyright 1985 by John Wiley & Sons, Ltd. Reprinted by permission.

case. However, due to a greater tendency to self-aggregation, the K value could not be determined.

The smaller Δδ values obtained for the chlorophylls compared to the pheophytins reveal the significant stiffening effect of the central magnesium in the porphyrin macrocycle, preventing large conformational changes. In both magnesium and nonmagnesium compounds, large Δδ values observed for P-1 CH_2, P-2 H, and P-3a CH_2 protons reveal the close proximity of this olefinic region of the phytyl group and the methoxycarbonyl group in the 10(*S*) form, in acetone. These large steric interactions are felt throughout the C-7 side chain and in ring IV. The largest Δδ is that of P-2 H and is attributed to the concerted anisotropic influence of the two ester carbonyl groups in close proximity to this phytyl methine proton. This large steric hindrance about the carbonyl in the 10(*S*) form accounts for the large difference in electron donor abilities of the prime and nonprime species.

The large difference between the Δδ observed for NH_I and NH_{III} provide evidence for the previous suggestion that the N-Mg bonds in the chlorophyll species are different in the R and S forms. The large N-H increments indicate the presence of more strain in these bonds in Chl **a**′ than Chl **a**, which accounts for the higher pheophytinization observed for the prime chlorophylls. This greater pheophytinization could be alternatively accounted for by the greater tendency to enolize in the prime form, redistributing π-electrons to ring V and hence weakening the N-Mg bonds.

Although this β-keto-ester function in chlorophylls is suspect to enolization, the keto/enol equilibrium remains firmly on the keto side, with only a small concentration of enol present. The presence of this enol is confirmed by the observed hydrogen exchange at C-10[46] and is implicated in the Molisch phase test[47] which establishes the integrity of ring V as an intermediate in the allomerization reactions of chlorophyll. Interest in this enol has been sustained by its proposed participation in the primary events of photosynthesis[48] and in photosynthetic oxygen evolution.[49] The enol has been observed by the formation of peripheral magnesium complexes of the pheophytins[50] and by being trapped by tetramethyl silylethers.[7,42,51] In both cases, the ring current-induced shifts of these complexes are less than their enol-free counterparts. The greatest chemical shift changes belong to those of the methine protons, implying a large decrease in the macrocyclic ring current due to redistribution of π-electrons to ring V in the stabilized enol.

F. CHLOROPHYLL PHOTOREDUCTION

The most fundamental photoreaction studied by ^1H NMR is the Krasnovskii photoreduction of chlorophyll.[52] The structure of the reaction product of Chl **a** has been shown to be the β, δ-dihydro-Chl **a**. The reaction in a sealed NMR tube, using H_2S (and D_2S) as reductant,[53] revealed the spectra of this porphodimethine, characterized by the high-field

shifts due to the loss of the "ring current" of the macrocyclic protons while those of the phytyl chain remain unchanged. More recently, Brereton and Sanders[54] have been examining the effect of illumination on BChl **a** in various solvents. In acetone solution and exposed to air, the color of the solution changed to that of a yellow-green chlorin. The product was deduced as being [2-acetyl]-Chl **a**,[55] and similar results were obtained in THF and ether, but the reaction was much slower. By contrast, illumination of methanol and pyridine solutions yielded no[2-acetyl]-Chl **a** product, but a radical cation. The presence of the radical was reflected in the ^{1}H NMR spectrum in acetone-d_6, which in ungassed acetone gave a spectrum which was differentially broadened, characteristic of rapid electron transfer between BChl and its radical cation. Brief illumination restored the differential broadening. This dehydrogenation occurs for the five-coordinate BChl, with the formation of a radical cation followed by loss of H^+ and H'. The latter step is prevented by sixfold coordination. This implies that the electron transfer requires the close proximity of two macrocycles, in the form of a transient dimer which is inhibited by sixfold coordination. A pronounced effect of solvation on the oxidation of chlorophylls has been observed by Shaber et al.[54a]

III. ^{13}C NMR OF CHLOROPHYLL MONOMERS

A. CHLOROPHYLLS

The utility of ^{13}C NMR spectroscopy in the investigation of the structure and properties of chlorophylls in solution has been well documented in previous reviews.[5-7] General studies of ^{13}C NMR spectra of chlorins have been reported by Lincoln et al.[56] and Smith and Unsworth.[57] The ^{13}C NMR spectra of Chl **a** itself has been given in a number of investigations.[58-63]

The original assignment of all 55 carbon atoms for Chl **a** was carried out by Boxer et al.[60] and Goodman et al.[64] The quaternary resonances were assigned by Boxer and the phytyl side chain by Goodman using phytyl acetate. The relatively low sensitivity of ^{13}C NMR meant that the initial investigations were carried out using biosynthetically ^{13}C-enriched compounds. The enrichment to 90[62,63] and 15%[60,61] ^{13}C levels increased the sensitivity and gave useful assignments via the C-C coupling. These couplings, however, frequently complicate the assignment. Reexamination of the ^{13}C chemical shifts by Lötjönen and Hynninen[58] revised the assignment of the β-pyrrolic C-6 and α-pyrrolic C-16 and C-17. The assignments of the methyl-Pheid **a** and methyl-pyro-Phe **a** were also found to be in error and were corrected by Wray et al.[65] and Smith et al.[57,66]

In order to reinvestigate more closely the factors influencing the ^{13}C chemical shifts, Hynninen et al.[59] have assigned the natural abundance chemical shifts for Chl **a** and several closely related derivatives. Table 8 shows the ^{13}C chemical shifts and their assignments for Chl **a** and its derivatives. The observed ^{13}C NMR shifts of Chl **a** are, like the ^{1}H shifts, extremely solvent dependent. A comparison of the ^{13}C chemical shifts measured in THF and acetone-d_6 solution is shown in Figure 4. A striking feature of these solvent effects is that the chemical shifts vary markedly in both magnitude and direction. The macrocyclic carbons experience downfield shifts, while the side-chain carbons are shifted slightly upfield upon substituting acetone for THF. As a general trend, the α-pyrroles experience larger $\Delta\delta$ than the β-pyrroles or methine carbons, except the β-pyrrole carbons of ring IV and C-6, which experience large upfield shifts. The most exceptional behavior is the large downfield shift (0.9 ppm) observed for C-2b, clearly indicating its participation in the macrocyclic π-system. These solvent effects are, as in the ^{1}H spectrum, dependent on axial ligation to the central magnesium. On going from the hexacoordinated species in THF to the pentacoordinated species in acetone, the magnesium lifts out of the plane of the macrocycle, affecting the chlorophyll π-system and hence the induced shift.

Comparison of the effects of the coordination of magnesium on the ^{13}C chemical shifts

TABLE 8
^{13}C Chemical Shifts of Chl a (a'), Phe a (a'), pyro-Chl a, and pyro-Phe a[a]

Carbon[b]	Chl a (a')[c]	Phe a (a')	pyro-Chl a	pyro-Phe a
1	135.5	132.1 (0.1)	135.2	131.7
2	139.0 (0.1)	[136.4 (−0.1)][e]	138.8	[136.1]
3	134.0	[136.0 (0.1)]	133.7	[135.7]
4	144.1	145.2	143.8	145.0
5	134.2	128.9 (−0.1)	[133.3]	128.0
6	131.9 (−0.4)	130.1 (−0.1)	[133.5]	131.4
7	51.6 (0.7)	52.1 (0.7)	52.1	52.6
8	50.0 (0.9)	50.8 (0.8)	50.1	50.7
9	189.3 (0.2)	189.2 (0.1)	195.2	194.7
10	66.2[d]	66.4[d]	49.2	48.4
11	154.0 (0.2)	142.2 (0.2)	153.5	141.6
12	148.0 (−0.1)	[136.5 (0.1)]	148.1	[136.3]
13	151.4 (0.2)	155.6 (0.1)	151.0	155.1
14	146.1	151.4 (−0.1)	145.9	151.2
15	147.7 (0.1)	138.5 (−0.2)	147.4	138.4
16	161.4 (0.7)	149.9 (0.6)	161.3	149.0
17	155.8 (−0.4)	162.1 (−0.2)	155.1	161.4
18	167.4 (0.6)	172.8 (0.3)	167.0	171.9
α	100.0	97.5	99.7	97.3
β	107.1 (0.2)	104.4	106.8	103.9
γ	106.2 (0.5)	106.8 (0.5)	106.4	107.2
δ	92.8 (0.1)	93.9	92.6	93.7
1a	12.6	11.9	12.6	12.0
2a	131.5	129.7	131.7	130.0
2b	118.9	122.1	118.6	121.9
3a	11.2	10.8 (−0.1)	11.2	11.0
4a	20.0	19.5	10.2	19.7
4b	18.0	17.4	18.1	17.6
5a	12.6	11.7 (−0.1)	12.6	11.5
7a	30.9	31.7 (−0.5)	31.0	31.6
7b	30.1	30.2 (−0.4)	30.7	30.0
7c	172.7	172.9	172.9	172.9
8a	23.9	23.3 (0.2)	23.8	23.3
10a	171.0 (1.1)	169.9 (1.2)		
10b	52.0	52.5 (−0.1)		
P1	61.3 (−0.2)	61.4	61.3	61.4
P2	119.4	119.5	119.5	119.5
P3	142.2 (0.1)	142.2 (0.1)	142.4	142.5
P3a	16.2	16.2	16.2	16.3
P4	40.4	40.5	40.5	40.5
P5	25.8	25.8	25.9	25.8
P6	37.4	37.4	37.4	37.4
P7	33.4	33.5	33.5	33.5
P7a	20.0	19.9	20.0	20.0
P8	38.0	38.1	38.2	38.1
P9	25.2	25.2	25.2	25.2
P10	38.0	38.1	38.2	38.1
P11	33.6	33.6	33.6	33.6
P11a	20.0	19.9	20.0	20.0
P12	38.0	38.1	38.2	38.1
P13	25.6	25.6	25.6	25.6
P14	40.1	40.2	40.2	40.2
P15	28.7	28.8	28.8	28.8
P15a	22.9	22.9	22.9	22.9
P16	23.0	23.0	23.0	23.0

TABLE 8 (continued)
^{13}C Chemical Shifts of Chl a (a'), Phe a (a'), pyro-Chl a, and pyro-Phe a[a]

[a] Solvent, tetrahydrofuran-d_8. Chemical shifts in ppm from internal TMS.
[b] See Figure 1 for numbering of the carbons.
[c] Chemical shifts for the prime isomer are obtained by adding values in parentheses to the chemical shifts.
[d] The C-10 line of the prime isomer was not detected, probably owing to its accidental coincidence with one of the solvent signals.
[e] Assignments in square brackets are tentative.

From Lötjönen, S. and Hynninen, P. H., *Org. Magn. Reson.*, 21, 757, 1983. Copyright 1983 by John Wiley & Sons, Ltd. Reprinted by permission.

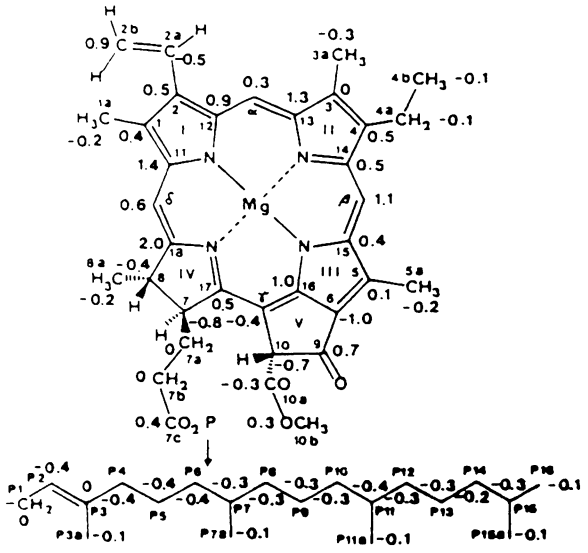

FIGURE 4. ^{13}C chemical shift increments resulting from changing the solvent from tetrahydrofuran-d_8 to acetone-d_6. Positive numbers represent downfield shifts. (From Lötjöhen, S. and Hynninen, P. H., *Org. Magn. Reson.*, 21, 757, 1983. Copyright 1983. Reprinted by permission of John Wiley & Sons, Ltd.)

can be seen by comparison of the Chl **a** and Pheid **a** shifts. This coordination effect was first investigated by Boxer et al.[60] Figure 5 shows the change in ^{13}C chemical shifts upon the complexation of Phe **a** with Mg. Although the new values differ markedly from those previously reported,[60] they follow similar trends. The α-pyrrole carbons of rings I and III experience large downfield shifts, whereas the signals from the corresponding carbons of ring II and IV are shifted upfield. The *meso* carbons show an upfield shift for the γ- and δ-positions, in contrast to previous studies where all the *meso* carbons moved downfield. Inclusion of the magnesium has little effect upon the phytyl side chain and only a small effect upon the other side chains. An exception is the prominent downfield shift for C-2a and upfield shift for C-2b, indicating, as in the case of the solvent effect, the substantial conjugation of the vinyl group with the macrocycle. The effect of Mg insertion has been previously discussed in terms of the energy level of the π-system and the nitrogen energy levels.[57,60,67]

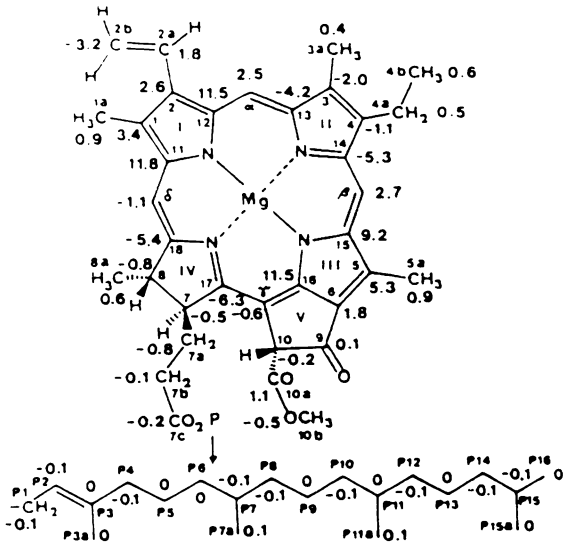

FIGURE 5. ^{13}C chemical shift changes on addition of Mg to Phe **a**. Positive values represent downfield shifts. (From Lötjöhen, S. and Hynninen, P. H., *Org. Magn. Reson.*, 21, 757, 1983. Copyright 1983. Reprinted by permission of John Wiley & Sons, Ltd.)

The effect of the addition of the 10-methoxycarbonyl upon the conformation of Chl is due to the large steric interaction with the C-7 side chain. Table 9 shows the observed effect on replacement of H by CO_2Me in pyro-Chl **a** and pyro-Pheid **a**. The $\Delta\delta$ values clearly indicate that the orientation of C-10 is critical. The observed $\Delta\delta$s for the 10(*S*) form (**a'**) are larger than those observed for the 10(*R*) (**a**) form, presumably due to the larger steric interactions present in this form, which are accommodated by alterations in the macrocyclic geometry. The deviations for the magnesium-free pheophytin 10(*S*) form are spread to a greater extent over the entire macrocycle than in the more rigid magnesium-containing pyrochlorophylls. The observed ^{13}C chemical shift effects are in complete agreement with those observed for the ^{1}H NMR of the epimers. Similar solvent and magnesium effects are seen for the ^{13}C chemical shifts of Chl **b**[68] (Table 10).

B. PROTONATION STUDIES

The titration of pyroPheid **a** with TFA in tetrahydrofuran reveals startling effects upon the ^{13}C chemical shifts.[69] Figure 6 shows the change in ^{13}C chemical shifts upon the addition of TFA. The C-13 and C-14 signals experience large upfield shifts (10 to 12 ppm) upon the addition of TFA, while the other shift changes are much smaller and in the opposite direction. After the addition of 15 Meq of TFA, the chemical shifts remain constant. The large shifts at C-13 and C-14 are due to the formation of a monocation in which the proton is attached to the nitrogen of ring II. This monocation formation redistributes the π-electrons and alters the conformation of the macrocycle, especially at the flexible ring IV, reflected in the downfield shift seen for these carbons. As seen previously, this change in π-electron density significantly affects the two vinyl groups, with the C-2b resonance moving 4 ppm downfield. This protonation effect has been previously seen in symmetrical porphyrins,[70,71] where the α-pyrrole carbons experience a 2-ppm upfield shift and the β-pyrrole carbons, a 3-ppm downfield shift. In pyro-Pheid **a**, however, the protonation shifts are specific to ring II, suggesting that the N-H protons are strictly localized. Any delocalization would cause protonation shifts at other α-carbons. The presence of the reduced ring IV prevents delo-

TABLE 9
Substituent Effects on Replacement of H by Methoxycarbonyl in pyro-Chl a and pyro-Phe a (Positive Numbers Represent Downfield Shifts)

Carbon	Δδ pyro-Chl a	Δδ pyro-Phe a	Carbon	Δδ pyro-Chl a	Δδ pyro-Phe a
1	0.3	0.4 (0.5)	α	0.3	0.2
2	0.2 (0.3)[a]	0.3 (0.2)[b]	β	0.3 (0.5)	0.5
3	0.3	0.3 (0.4)[b]	γ	−0.2 (0.3)	−0.4 (0.1)
4	0.3	0.2	δ	0.2 (0.3)	0.2
5	0.9[b]	0.9 (0.8)	1a	0.0	−0.1
6	−1.6 (−2.0)[b]	−1.3 (−1.4)	2a	−0.2	−0.3
7	−0.5 (0.2)	−0.5 (0.2)	2b	0.3	0.2
8	−0.1 (0.8)	0.1 (0.9)	3a	0.0	−0.2 (−0.3)
9	−5.9 (−5.7)	−5.5 (−5.4)	4a	−0.2	−0.2
10	17.0[c]	18.0[c]	4b	−0.1	−0.2
11	0.5 (0.7)	0.6 (0.8)	5a	0.0	0.2 (0.1)
12	−0.1 (−0.2)	0.2 (0.3)[b]	7a	−0.1	0.1 (−0.4)
13	0.4 (0.6)	0.5 (0.6)	7b	−0.6	0.2 (−0.2)
14	0.2	0.2 (0.1)	7c	−0.2	0.0
15	0.3 (0.4)	0.1 (−0.1)	8a	0.1	0.0 (0.2)
16	0.1 (0.8)	0.9 (1.5)			
17	0.7 (0.3)	0.7 (0.5)			
18	0.4 (1.0)	0.9 (1.2)			

[a] The numbers in parentheses represent the effects of the substituent above the plane of the macrocycle ([10*S*]epimer), if they differ from the effects of the substituent below the plane ([10*R*]epimer).

[b] Based on tentative assignment.

[c] Determination of the effect in the (10*S*) form was not possible owing to the coincidence of the signals of C-10 and solvent.

From Lötjönen, S. and Hynninen, P. H., *Org. Magn. Reson.*, 21, 757, 1983. Copyright 1983 by John Wiley & Sons, Ltd. Reprinted by Permission.

calization through ring II, which is reflected in the minor effect upon C-3 and C-4 on protonating the ring II nitrogen. Consequently, the C-3 to C-4 bond in pyropheophorbide is almost a pure double bond isolated from the conjugated system. Figure 7 shows the dominant resonance structure of the free base phorbin.

C. BACTERIOCHLOROPHYLLS

Analysis of the ^{13}C spectra of Chl **a** and Chl **b** was aided by ^{13}C enrichment. The difficulty in enriching the bacteriochlorophylls has restricted research into their ^{13}C spectra. Recently, Sanders et al., using a mixed-solvent system, methanol:pyridine (1:4), in order to stabilize the concentrated solution, assigned the ^{13}C chemical shifts of BChl **a**, using the power spectrum display mode.[72] The assignment was based partly upon those for Chl **a** by Boxer et al.[60] The spectral assignment was corrected by Oh-hama et al.[74] The spectra of BChl **a** formed by *Rp. sphaeroides* in the presence of [2-^{13}C] glycine produces ^{13}C enrichment at the four *meso* carbons and also at the four α-pyrrole carbons C-12, C-14, C-16, and C-17. The assignment of these enriched positions was aided by long-range selective proton decoupling. Table 11 shows the ^{13}C chemical shifts of BChl **a**. The ^{13}C chemical shifts of BChl **a** are generally similar to Chl **a** except that there are substantial chemical shift differences in rings I and II.

TABLE 10
The Observed ^{13}C Chemical Shifts for Chl b and Relative Derivatives

C atom	Chl b	Chl b	Phe b	pyro-Phe b
	$CDCl_3(H_2O)$	Acetone-d_6	$CDCl_3$	$CDCl_3$
9	190.26	190.62	189.52	195.64
3a	187.66	187.69	187.12	187.01
7c	173.55	173.42	173.37	173.45
10a	170.79	171.05	169.48	—
18	170.79	171.46	173.99	173.07
16	163.90	164.38	150.81	149.91
17	158.71	159.70	164.15	162.98
11	157.51	157.54	143.51	142.89
4	155.87	155.79	158.80	158.14
12	149.85	150.05	136.93	136.43
13	149.23	149.45	150.73	150.13
15	148.76	149.45	137.87	137.56
14	142.64	143.41	146.80	146.25
2	140.72	141.06	137.56	137.01
5	139.28	138.87	132.20	131.02
1	136.24	136.98	132.20	131.79
6	131.27	132.78	129.74	129.95
3	129.71	131.22	132.47	132.09
2a	129.79	130.94	128.64	128.75
2b	120.80	120.80	123.34	122.99
β	111.06	111.37	106.45	105.76
γ	104.20	105.96	105.08	105.63
α	102.96	103.59	101.25	100.62
δ	92.96	93.96	93.33	93.02
10	64.96	65.91	64.73	47.92
10b	52.76	52.84	52.98	—
7	50.46	51.45	51.58	52.02
8	49.22	50.03	50.27	50.11
7a	31.06	31.28	31.33	31.19
7b	29.74	30.18	29.82	29.71
8a	23.34	23.76	23.10	23.02
4a	19.18	19.55	18.56	18.53
4b	18.89	19.55	19.05	19.03
1aʃ	12.60	12.64	12.00	11.95
5aʃ	12.22	12.38	11.95	11.75
7d	—	—	51.75	51.75

Note: All shifts relative to TMS.

D. OTHER NUCLEI

Very few NMR studies have been carried out with other nuclei. The assignment of the ^{15}N chemical shifts has been made for Pheid **a** and Chl **a** by 95% enrichment, incorporated by biosynthesis.[60] In addition to ^{15}N, the ^{2}H NMR spectra of Chl **a** has been recorded for Chl **a**-$\mathbf{d}_{72}$ and methyl-Pheid **a**-$\mathbf{d}_{35}$.[75] This work is reported in previous reviews.[7]

IV. NMR SPECTRA OF CHLOROPHYLL DIMERS AND OLIGOMERS

In nonnucleophilic solvents, the ^{1}H NMR spectra of Chls are substantially different from those observed in nucleophilic solvents. In the absence of an external ligand, the vacant

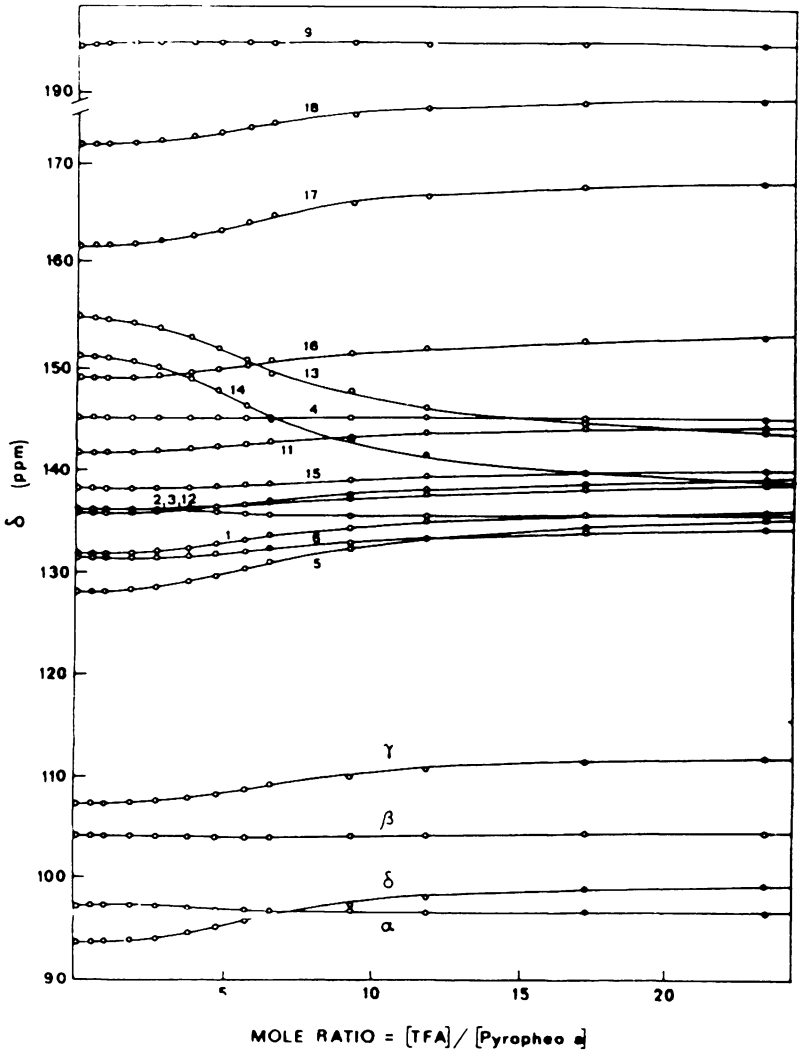

FIGURE 6. ^{13}C NMR titration of pyro-Phe **a** in tetrahydrofuran with trifluoroacetic acid. (From Lötjönen, S. and Hynninen, P. H., *Org. Magn. Reson.*, 22, 511, 1984. Copyright 1984. Reprinted by permission of John Wiley & Sons, Ltd.)

coordination sites on the central magnesium are satisfied by a second chlorophyll molecule which coordinates directly, using a carbonyl function, or indirectly, via a water molecule with hydrogen bonds, to the carbonyl. This aggregation is determined by the solvent, the concentration, and the temperature. In polarizable nonnucleophilic solvents, e.g., chloroform or carbon tetrachloride, Chl **a** is predominantly in the dimeric form, whereas in nonpolarizable solvents, e.g., benzene, or octane, it is present as large oligomers — $(\text{Chl } \mathbf{a})_n$ where $n > 20$. Brereton and Sanders[76] found that, for BChl **a** in wet benzene, the water breaks up these large oligomers into smaller dimers and trimers.

The spectra of Chl **a** in noncomplexing solvents shows considerable broadening of many of the resonances. In 0.04 *M* solution in d_8-octane, virtually all traces of fine structure are absent.[14] In $CDCl_3$, certain resonances broaden considerably; thus, even at 500 MHz, the observed spectrum is not easily assigned.[77] This line broadening is probably due to exchange broadening between the monomer and aggregate, especially in concentrated solutions and hydrocarbon solvents. The presence of a small quantity of Chl π-cation radicals could also

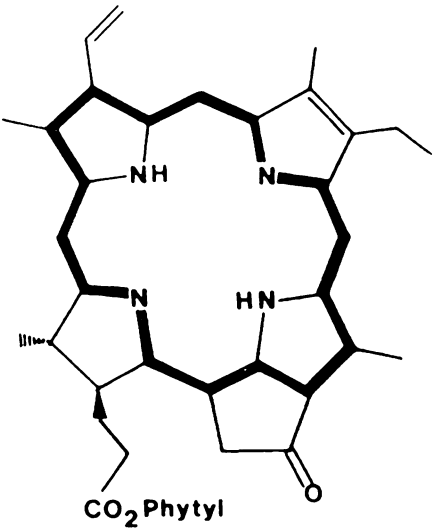

FIGURE 7. Dominant resonance structure of the free base phorbin. (From Lötjönen, S. and Hynninen, P. H., *Org. Magn. Reson.*, 22, 511, 1984. Copyright 1984. Reprinted by permission of John Wiley & Sons, Ltd.)

contribute to the broadening, being greatest at the *meso* protons since the adjacent carbon atoms have the largest unpaired spin density (seen in Chl **b**[78]). A further possibility is chemical shift anisotropy, which is most pronounced at the *meso* positions, and greater broadening is observed at 500 MHz compared to 100 MHz. However, calculation of this line broadening using reasonable values for the anisotropy gave much less than the observed line broadening.[79] It is very likely that a number of factors contribute to the line broadening, which, whatever the cause, precludes the assignment of the aggregate spectra and accurate values of the complexation shift being obtained directly. It is possible to ascertain the chemical shifts of the dimeric species by a titration procedure in which ^1H chemical shifts are recorded as a function of the Chl **a**/nucleophile ratio. This dissociation of the dimer to the monomer and subsequent complexation with the ligand can be defined by the equilibria in Figure 8.

A. CHLOROPHYLL COMPLEXATION SHIFTS

Numerous research workers have studied the aggregation shifts of Chl **a**[7] ($\Delta\delta$ = δ dimer − δ monomer), the most recent being that of Abraham et al.,[77] which at the high-field strengths used allowed the assignment of many more resonances and thus gave a more complete aggregation map than previous work. In order to prevent the presence of any aggregates larger than the dimer, the concentration of Chl **a** solution in chloroform was 2.8 m*M*. Ballschmiter et al.[80] showed by vapor-phase osmometry that Chl **a** exists as a dimer in carbon tetrachloride down to very low concentrations, with higher aggregates forming at concentrations $>10^{-2}$ *M*. This dimeric solution was titrated with methanol (Figure 9 shows the change in chemical shift with the addition of mole equivalents of methanol). Extrapolation of the titration curves gives the complexation shifts in the dimer. The observed K_3 value for this titration was 7.0 l/mol, which compares with 19.4 l/mol observed from infrared measurements for the titration of Chl **a** with tetrahydrofuran in carbon tetrachloride. Katz et al.[6] quote values of 58 l/mol for Chl **a** methanol titration and 3.5×10^3 l/mol for Chl **a** pyridine titration in carbon tetrachloride.

The observed aggregation shifts are in good agreement with the original values of Closs

TABLE 11
^{13}C Chemical Shifts in BChl a[a]

Assignment	Chemical shift	Assignment	Chemical shift
2a	197.6	7	49.0
9	187.5	8	48.0
7c	171.7	3	46.7
10a	170.7		38.5[b]
17	166.1[b] (160.2)[c]	P4, P6, P8	38.2, 38.5[b]
18	164.9[b]	P10, P12, P14	36.2, 35.3[b]
6			35.3
11	150.2	P7, P11, P15	31.6, 31.1[b]
16	143.8 (158.1)[c]		31.4
15	147.9		
12	147.9 (149.7)[c]		
P3	141.2	7a, 7b, 4a	31—27
14	140.6 (151.7)[c]		
13	140.6	P5, P9, P13	23.6, 23.8[b]
5	135.1		23.2
1	127.6	3a, 8a	21.2, 21.2[b]
2	122.3		
P2	117.2		
γ	107.1 (109.4)[c]	P7a, P11a, P15a	21.2, 18.3[b]
β	99.9 (101.6)[c]	P3a	14.1
α	97.6 (99.0)[c]	1a	12.0
δ	94.2 (95.6)[c]	5a	10.3
10	65.0	4b	9.1
P1	59.8		
4	54.0		
10b	50.8		

[a] 1 *M* concentrated in acetone/methanol.
[b] Assignments unknown.
[c] Corrected assignments, Ref. 74.

From Brereton, R. G. and Sanders, J. K. M., *J. Chem. Soc. Perkin Trans. 1*, 435, 1983. With permission.

$$Chl_2 \overset{K_1}{\rightleftharpoons} 2\ Chl$$

$$Chl + L \overset{K_2}{\rightleftharpoons} ChlL$$

$$Chl_2 + 2L \overset{K_3}{\rightleftharpoons} 2\ ChlL$$

$$K_3 = K_1K_2$$

FIGURE 8. Equilibria for chlorophyll disaggregation.

et al.[13] The observed differences are due to the presence of higher aggregates in these more concentrated solutions, clearly seen for those protons with the largest complexation shifts, in particular 10-H, 5-Me, and 8-Me. The limiting value of the complexation shift for a large aggregate is slightly more than twice the complexation shift in the dimer. The large shifts observed for 10-H, particularly for the measurement in carbon tetrachloride solution, are almost twice the present values, strongly suggesting the presence of larger aggregates. (Table 12 shows the observed complexation shifts and the calculated shifts for various structures [see later discussion].)

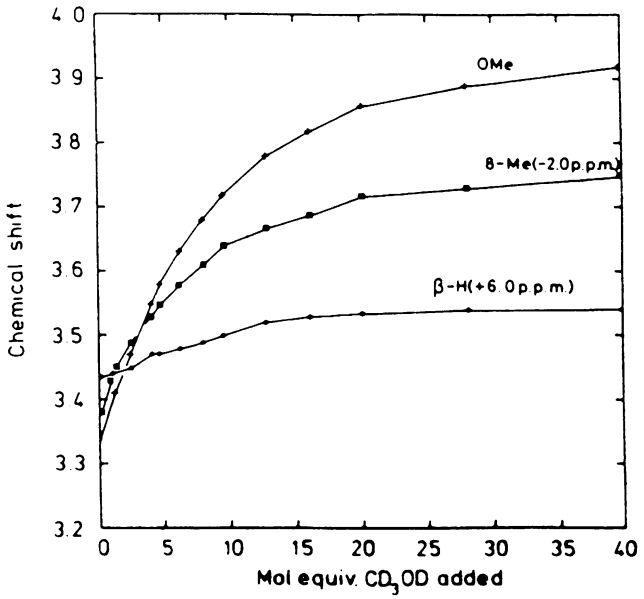

FIGURE 9. Titration of Chl **a** in $CDCl_3$ with CD_3OD. Chemical shifts vs. mol equiv. CD_3OD added. (From Abraham, R. J., Goff, D. A., and Smith, K. M., *J. Chem. Soc. Perkin Trans. 1*, 2443, 1988. With permission.)

The aggregation shifts yield valuable structural information about the dimer geometry. These shifts can be accurately related to the dimer geometry due to the development by Abraham et al.[81,84] of the double dipole model for the chlorophyll ring current. This model enables the aggregation shifts to be accurately calculated for various proposed dimeric structures and the dimeric structure obtained by comparison with the observed shifts. Abraham et al., using this model, have examined all the previous proposed dimeric models (Figure 10 shows the geometry of the proposed models).

Note that this is a *dynamic* equilibrium, not a static one, and all of these structures could, in principle, be in equilibrium in solution.

B. CHLOROPHYLL AGGREGATE STRUCTURES

The one-dimensional polymer was suggested by Chow et al.,[21] by comparison with the crystal structure of ethyl-Chlid **a** dihydrate, where the chlorophyll molecules are linked by a hydrogen-bonded chain involving both the C-7 and C-10 ester C=O groups, and also the C-9 keto group (Figure 10A), as a possible model for the organization of antenna chlorophylls. The calculated shifts for this model show no relationship with the observed model (Table 12). This negative result illustrates very clearly the profound differences in chlorophyll aggregation between the solid and solution states. The Shipman model[85] (Figure 10B), was proposed as a model for the structure of the special pair of Chl **a** and was based upon infrared and visible spectra of an ethanol adduct of Chl **a** in toluene. In this proposed dimer, the two equivalent Chl **a** molecules are held together by two ROH ligands, each of which is simultaneously coordinated to the magnesium atom of one Chl **a** molecule and hydrogen bonded to the C-9 keto function of the other Chl, with an interplane separation of about 3.6 Å. In this model, rings C and E are above the same rings in the neighboring molecule and hence would experience a large ring current shift, but the C-10a ester methoxy group, being *exo* to the dimer structure, would experience a very small shift. The calculated ring current shifts (Table 12) for this structure show the C-5-Me experiencing a very large shift and the

TABLE 12
Observed and Calculated Complexation Shifts (Δδ) for Chl a

Proton	Observed shifts (monomer-dimer)			Calculated shifts					
	This work	a	b	c	d	e	f	g	h
Meso	0.06	0.08	0.24	0.13	0.10	0.02	0.02	0.00	0.06
Meso β	0.10	0.18	0.22	0.06	0.31	0.24	0.36	0.22	0.07
Meso δ	0.08	0.13	0.07	0.06	0.09	0.03	0.12	0.16	0.03
1-Me	0.01	0.03	0.05	0.33	0.06	0.03	0.05	0.00	0.07
3-Me	0.03	0.07	0.11	0.08	0.11	0.02	0.05	0.02	0.06
5-Me	0.64	0.83	0.90	0.47	3.04	0.58	0.35	0.43	0.59
8-Me	0.39	0.42		0.12	0.02	0.02	0.49	0.31	0.29
8-H	0.43			0.10	0.12	0.01	0.44	0.37	0.42
10-H	1.26	1.85	2.05	0.06	0.31	1.56	1.27	1.34	1.32
4a-CH_2	0.01	0.08		0.09	0.05	0.11	0.03	0.01	0.07
4b-Me	0.02			0.13	0.45	0.10	0.06	0.01	0.01
10-OMe	0.64	0.72	0.61	0.05	0.04	1.28	0.75	0.60	0.50
P-2	0.30								
P-4-CH_2	0.03								
P-3a-Me	0.14								

[a] Methyl chlid (0.08 *M* in $CDCl_3$) titrated with methanol (Ref. 17).
[b] Chl **a** (0.06 *M* in CCl_4) titrated with [$^2H_5$]pyridine (Ref. 6).
[c] The Strouse model, displacement coordinates −5.0, 6.8, −4.0 Å, no rotation.
[d] The Shipman model, displacement coordinates −5.0, −6.0, −3.6 Å, rotated −105°.
[e] The skew dimer, displacement coordinates 2.6, −8.4, 0.0 Å, orthogonal position.
[f] The Fong model, displacement coordinates 0.0, 3.6, 5.0 Å, C_2 symmetry.
[g] The piggyback model, displacement coordinates 0.0, −4.5, 6.0 Å, rotated 205°.
[h] The back-to-back model, displacement coordinates 3.4, −5.8, 4.8 Å, inverted molecule.

From Abraham, R. J., Goff, D. A., and Smith, K. M., *J. Chem. Soc. Perkin Trans. 1*, 2443, 1988. With permission.

C-10a ester group experiencing a very small shift, and these calculated shifts are not in agreement with the observed shifts (Table 12).

The skew Chl dimer was originally proposed on the basis of circular dichroism[86] and NMR studies[87] with an angle between the Chl planes of 40°. This early suggestion was not generally accepted, but was revived recently by Kooyman and Schaafsma[88] from their measurements of nuclear relaxation times and chemical shifts. In their model, the two Chls are orthogonal, with the C-9 C=O of one Chl coordinating directly to the magnesium of the other (Figure 10C). The only protons observed were those lacking any internal rotation, and thus only the relaxation times of the three *meso* protons was measured. Due to the underdetermined geometry obtained using only these three values, Kooyman and Schaafsma used ring current calculations to further define the dimer geometry. The calculated shifts for this model (Table 12) do, indeed, follow the observed trends, especially for the three *meso* protons, which is not unexpected since they were the only protons measured. However, for the other protons, the calculated shifts are very different from those observed. The central problem in the skew dimer is that the C-9 keto group is sterically shielded in the Chl plane by the 5-Me and the 10-α ester groups, and any attempt to coordinate directly to the magnesium of the adjacent molecule would result in large steric interactions, which, with the poor agreement between the observed and calculated shifts, dismisses this structure.

The original model proposed for the Chl **a** dimer by Fong and Koester[89] is one in which the C-10 carbonyl ester group of both molecules coordinates with the magnesium of the other Chl. In this molecule, however, for the C-10 C=O oxygen to approach close enough

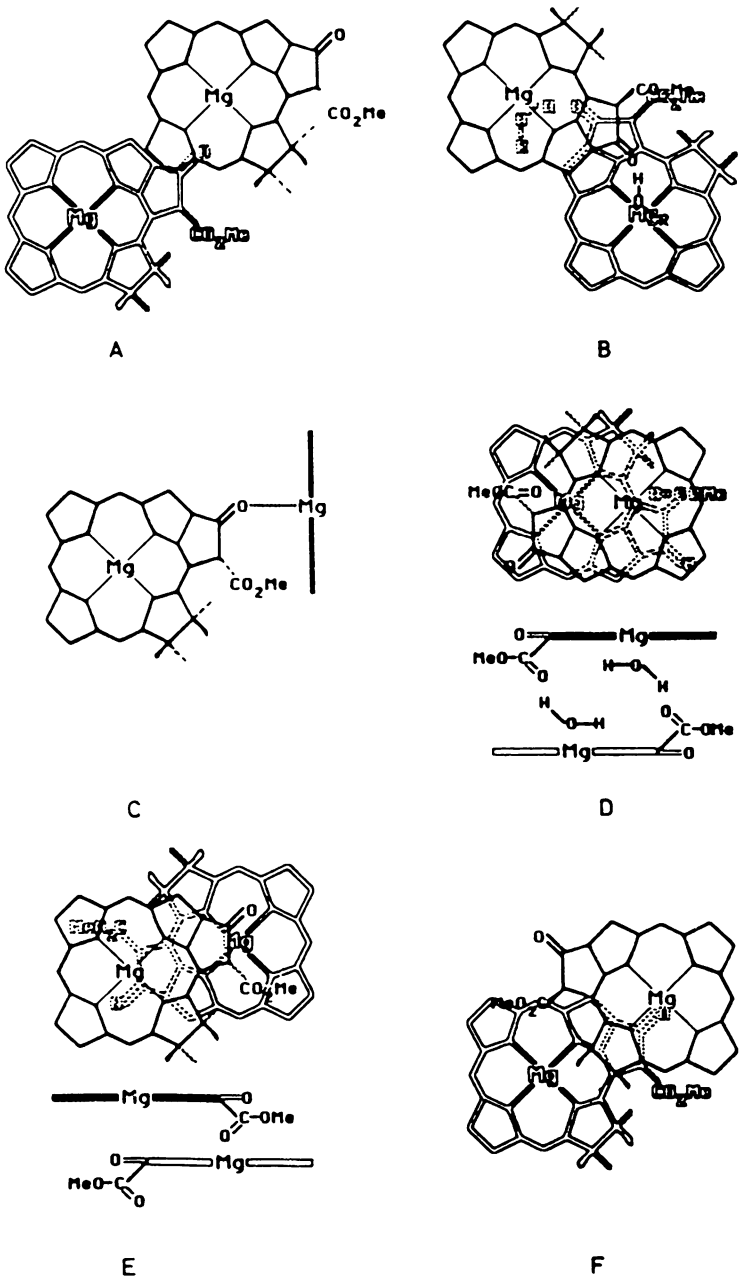

FIGURE 10. Proposed models for the Chl **a** dimer. (A) The Strouse model; (B) the Shipman model; (C) the skew model; (D) the Fong model; (E) the piggyback model; (F) the back-to-back model. (From Abraham, R. J., Goff, D. A., and Smith, K. M., *J. Chem. Soc. Perkin Trans. 1*, 2443, 1988. With permission.)

to be directly bound to the magnesium, the protons of the methoxy group would experience quite unacceptable steric repulsions. The more reasonable model suggested by Fong and Koester was one where there is a bridging water molecule between each C-10 carbonyl and the magnesium, which gives an interplane separation of 5 to 6 Å (Figure 10D). The calculated shifts for this model reproduce the general trends of the observed shifts reasonably well. The problem with the Fong model is that it cannot explain the similar complexation shifts

for the pyro-Chl **a** series where the critically important C-10 methoxycarbonyl group is absent. A Chl **a** derivative in which the carbomethoxy group is present but the 9-keto group is reduced to a CH_2 has been synthesized by Scheer.[7] It was found that, compared to Chl **a**, the aggregation shifts for 9-desoxomesochlorophyll **a** were considerably less, dismissing the Fong model as the major dimeric species.

Two models proposed by Abraham et al. to explain the observed aggregation shifts were the "piggyback" model and the "back-to-back" model, based upon earlier studies.[82,83] In the piggyback model (Figure 10E), the unsymmetrical dimer has a head-to-tail conformation, with both molecules facing the same way. Using the 12 dimer shifts observed, the optimization of the model converged to a good, single solution (Table 12 shows the calculated shifts and displacement coordinates). The estimated interplane separation of 6 Å is far too large to allow direct coordination, even assuming that the Mg lies 0.4 Å out of the plane. Inspection of this model reveals that the C-10 carbonyl points directly at the central Mg of the adjoining molecule. This geometry would appear to be optimum for a coordinating water molecule bound to the magnesium-to-hydrogen bond to the carbonyl of the C-10 group. Although the C-9 C=O appears directly over the Mg atom, it is too distant to be directly involved, and therefore the aggregation would need to be via at least one water molecule linking the C-9 keto function with the Mg of the adjacent molecule.

The final proposed model is the back-to-back dimer where, unlike the face-to-face Fong model with both C-10 methoxy carbonyl groups *endo* to the structure, both ester functions are *exo*. Optimization of this model (Table 12) gave a marginally better agreement than any other model, with an interplane separation of 4.8 Å, but with both molecules not rotated, simply inverted and displaced (Figure 10F). In this model, the C-9 keto function is situated over the central magnesium, while the other is far removed, with the C-10 ester groups of both Chls being *exo* and playing no part in the binding. In this structure and the piggyback structure, the carbonyl group of the C-7 propionate group can approach and be involved in binding to the magnesium. This is strongly supported by the observed complexation shifts of the phytyl group. The advantage of the back-to-back model is that it can account for the similar behavior in pyroChl **a**, as well as previous infrared data. In nonpolar media, the intensity of the free C=O band of Chl **a** at 1695 cm^{-1} attributed to the C-9 C=O diminishes by half and a new band appears at 1652 cm^{-1}. This result can be accounted for by the back-to-back model, where, upon aggregation, only one C-9 carbonyl group is involved with binding, while one is not involved. This free C-9 keto function and both free C-10 esters enable this dimeric seed to easily form larger aggregates.

C. METHYL PYROCHLOROPHYLLIDE a

At room temperature in a solution containing both the dimer and monomer Chl **a**, only one set of resonances can be observed, implying an averaging process on the ^1H NMR time scale. Katz and Brown[7] observed, for pyro-Chl **a**, sharp resonances in the ^1H NMR spectra at room temperature, while decreasing the temperature lead first to an increase in broadening, but below $-35°C$, the lines gradually sharpened and split into a multitude of resonances, typical of a slow exchange process. As a consequence of this unusual result, Abraham et al.[90] investigated the aggregation effects observed in methyl-pyro-Chlid **a**. The aggregation of pyrochlorophyll was previously observed by Katz and Brown,[7] where it was found, by NMR and infrared, that this species had behavior identical to Chl **a**. Indeed, the infrared measurements gave a larger equilibrium constant for the dimerization in pyro-Chl **a** than for Chl **a**.[7]

Titration of a methyl-pyro-Chlid **a** chloroform solution (concentration $<10^{-2}$ *M*) with pyridine-d_5 produced chemical shifts for the monomeric species identical with those observed upon the addition of excess methanol-d_4. The equilibrium of Figure 8 does not take into account a second molecule of pyridine which could also complex with the Mg. (The equi-

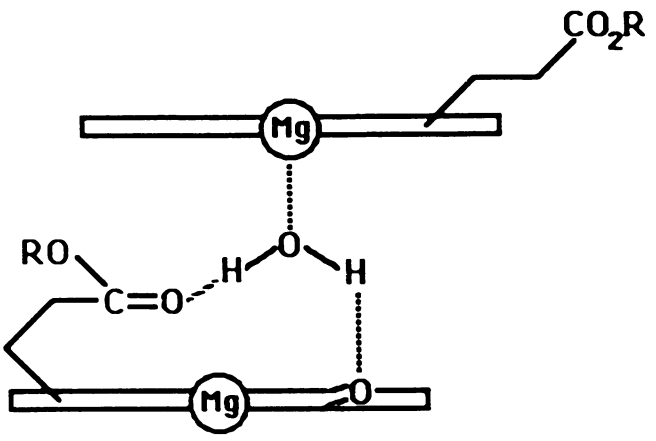

FIGURE 11. Proposed hydrogen bonding network in methyl-pyro-Chlid **a** dimer. (From Abraham, R. J., Rowan, A. E., Goff, D. A., Mansfield, K. E., and Smith, K. M., *J. Chem. Soc. Perkin Trans. 2*, 1633, 1989. With permission.)

librium constants for the first and second dissociation of pyridine in magnesium porphyrin dipyridinates are about 2000 and 0.1 l/mol, respectively.[91] It can be assumed that in this solution, from the identical chemical shifts in methanol and the weak binding coefficient of a second pyridine group, the final monomeric species has only one axially bound pyridine ligand. Analysis of the observed titration curves for pyridine and methanol gave values for K_3 of 260 and 13 l/mol, respectively. This compares with a value for K_3 of 19.4 l/mol observed for the titration of pyro-Chl **a** in carbon tetrachloride with tetrahydrofuran.

The observed aggregation shifts were found to be very similar to those seen for Chl **a**. The only difference in the complexation shifts observed in the pyro-Chl **a** and Chl **a** are those of the flexible ring IV, C-8H, and C-8Me. The overall similarity of the complexation shifts strongly support identical binding mechanisms in both molecules, and clearly exclude any significant involvement of the C-10 group in the Chl **a** dimer bonding. This confirms the similar conclusions of Katz and Brown[7] and constitutes strong evidence against the Fong model. (Figure 11 shows an aggregation map of the complexation shifts for methyl-pyro-Chlid **a** and, in brackets, Chl **a**.) The observed aggregation shifts differ from those reported by Katz and Brown in the more aggregating carbon tetrachloride solution.[7] There is no simple relationship between the two sets of data. The higher-field shifts observed by Katz in the more aggregating solution suggests that larger aggregates were present which have a layered structure (otherwise, the complexation shifts would not be further to higher field) which is not a direct extension of the dimer structure.

The observed complexation shifts of methyl-pyro-Chlid **a** were so similar to those of Chl **a** that similar dimer geometries were assumed; hence, only three proposed models for the methyl-pyro-Chlid **a** dimer were considered: the Fong model, the piggyback model, and the back-to-back model. Of these models, only two accurately reproduce the observed shifts — the piggyback and the back-to-back model. (Table 13 shows the observed and calculated complexation shifts.) Examination of these shifts reveals a large complexation shift for the $C\text{-}7_d$ methyl protons. In Chl **a**, the analogous proton also experiences a large aggregation shift. This strongly suggests that the methyl protons in methyl-pyro-Chlid **a** are in the shielding cone of the ring current, and thus the propionate side chain is folded into the dimer rather than extended into the solvent, which would produce a low-field, rather than high-field, complexation shift. The large aggregation shifts for this propionate side chain suggest the involvement of both the C-7 and C-9 carbonyl functions. The estimated interplane

TABLE 13
Observed and Calculated Complexation Shifts (Δδ) for methyl-pyro-Chlid a

	Obs.	a	b	c
Meso β	0.15	0.23	0.25	0.26
Meso α	0.08	−0.04	−0.02	−0.01
Meso γ	0.09	0.00	0.03	0.01
Vinyl 2a	0.03	−0.03	−0.03	−0.02
Vinyl 2b	0.01	−0.03	−0.03	−0.01
Vinyl 2b′	−0.01	−0.03	−0.03	−0.01
10-CH_{cis}	1.22	1.30	1.24	0.67
10-CH_{trans}	0.98	0.74	0.94	1.21
8-H	0.23	0.11	0.13	0.09
7-H	0.33	0.44	0.43	0.38
4a-CH_2	0.02	−0.01	0.01	0.02
7d-OMe	0.70	—	—	—
5-Me	0.66	0.65	0.64	0.60
1-Me	0.01	−0.04	−0.03	−0.02
3-Me	0.01	−0.04	−0.03	−0.02
4b-Me	0.02	0.05	0.00	0.06
8-Me	0.10	0.16	0.07	−0.03

[a] The back-to-back model, displacement coordinates 4.1, −5.2, 5.6 Å, rotated −30°, inverted molecule.
[b] The piggyback model, displacement coordinates 0.8, −5.9, 5.9 Å, rotated 215°.
[c] The Fong model, displacement coordinates −2.1, 5.4, 6.5 Å, C_2 symmetry.

From Abraham, R. J., Rowan, A. E., Goff, D. A., Mansfield, K. E., and Smith, K. M., *J. Chem. Soc. Perkin Trans. 2*, 1633, 1989. With permission.

separation for both dimer models (5 to 6 Å) is far too large for direct linkage; thus, it was suggested that the bonding mechanism involved bridging hydrogen bonds between a water molecule coordinated to the magnesium and other ligands. (Water was not rigorously removed in this study and was observed in the ^1H spectra. Addition of excess water was found to only partially dissociate the dimer).

The incorporation of a water molecule into the proposed dimer structure allows, in both proposed models, a dimer orientation such that both the C-7_d and C-9 carbonyls can be oriented to hydrogen bond to the attached water molecule. This results in a hydrogen bond to the flexible C-7_d carbonyl group which is almost linear, and a hydrogen bond to the C-9 carbonyl which is more orthogonal. (The proposed hydrogen bonding network is shown in Figure 11.) This proposed hydrogen bonding network is very similar to that found in the crystal structure of methyl pyrochlorophyllide **a** monohydrate monoetherate.[92] Here, the water molecule again forms a bifunctional bridging network, coordinating to the Mg of one molecule and hydrogen bonding to both the C-9 keto function of a neighboring methyl-pyro-Chlid **a** molecule and to the ether oxygen. The distance between this ether oxygen and the ring atom of the methyl-pyro-Chlid **a** molecule via the O···H–O···Mg linkage is 5.8 Å, very similar to the separation of the porphyrin planes for both models.

The major difference between the two models is the orientation of the C-7 propionate side chains, which in the "back-to-back" model are both *endo*, but in the "piggyback" one is *endo* and one is *exo*. In the back-to-back model, both propionate carbonyls could theoretically be involved in bonding, but this would incur large steric constraints as both

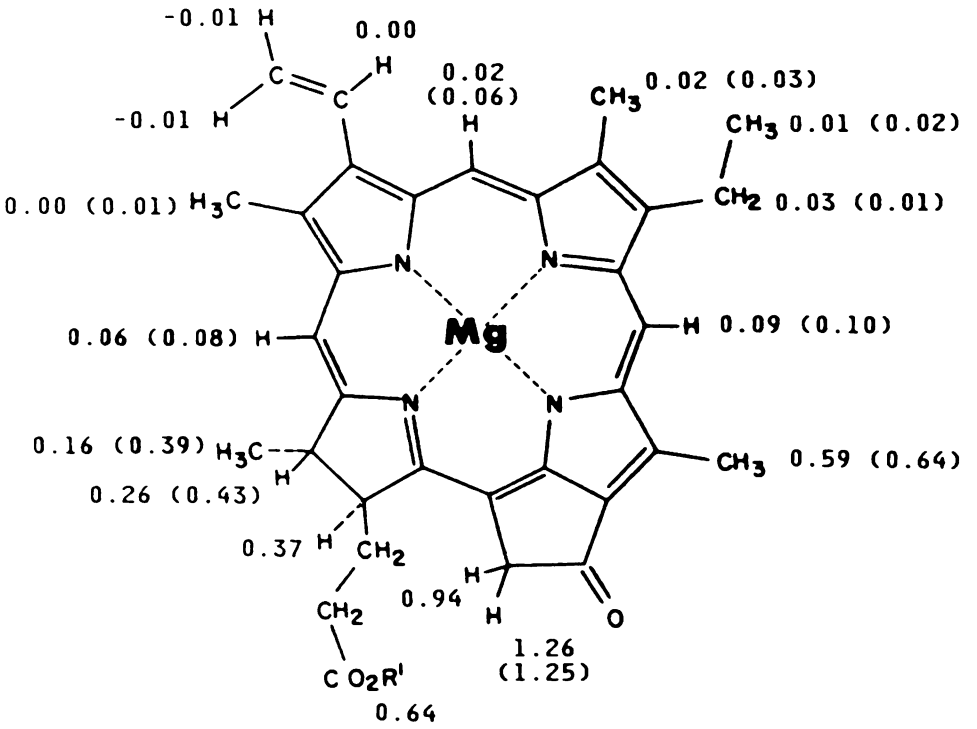

FIGURE 12. Aggregation map for methyl-pyro-Chlid **a** and Chl **a** titrated against CD_3OD. (From Abraham, R. J., Rowan, A. E., Goff, D. A., Mansfield, K. E., and Smith, K. M., *J. Chem. Soc. Perkin Trans. 2*, 1633, 1989. With permission.)

propionate groups are in the same region of the dimer. Both models can form larger aggregates due to the available C-9 keto. In the piggyback model, the attachment of a third Chl molecule would follow the same mechanism proposed for the dimer, whereas in the back-to-back model with both C-7 propionate groups, *endo* aggregation would have to occur by a slightly different mechanism.

Support for the involvement of both the C-9 and C-7_d carbonyl functions in the dimeric structure comes from the ^{13}C NMR aggregation shifts of Chl **a**. (Figure 12 shows an aggregation map of the observed ^{13}C NMR complexation shifts.) The carbon atoms in the dimer molecule will experience identical ring currents, compared to the protons. Thus, the three carbonyl carbon atoms of Chl **a** all experience high-field ring-current shifts. However, coordination interactions of a carbonyl group produce an additional downfield shift of the carbonyl carbon of up to several ppm. The complexation shifts of the C-9, C-10_a, and C-7_d carbons in Chl **a** were found to be -2.29, 0.40, and -0.98 ppm, respectively. This clearly implicates both C-9 and C-7_d in the bonding process, but not, as anticipated, C-10_a. The much larger negative shift of the C-9 carbonyl is due to its conjugation with the macrocyclic ring.

Upon cooling the solution of methyl-pyro-Chlid **a** in chloroform, no general line broadening characteristic of an exchange process was observed, even down to $-30°C$ in chloroform and $-60°C$ in methylene chloride, in contrast to that seen for pyro-Chl **a** by Katz and Brown.[7] Instead, upon cooling, a gradual change in peak positions occurs. (No observed temperature dependence was seen for the disaggregated species at the same concentration.) The resonances of ring D, C-7H, C-8H, and C-8-Me all move to lower field upon decreasing the temperature. The C-7 propionate signals also appear to follow this pattern, although they cannot be individually assigned, and the C-7_d methyl signal moves downfield with a larger

temperature dependence (0.32 ppm) (confirmed by deuteration at this position). The C-5-Me, however, shows an opposite temperature dependence upon moving to high field. All other protons show no temperature dependence. (Figure 13 shows the observed temperature effects upon the methyl-pyro-Chlid **a** dimer.)

The involvement of the C-7 propionate group in the dimeric species may account for this intriguing behavior. Upon cooling, the percentage of aggregate in the dimer-monomer equilibria increases, causing an upfield shift experienced by C-5-Me. The downfield shifts seen for the C-7 propionate group and neighboring ring IV protons can be accounted for by a competing intermolecular hydrogen-bonding interaction. As the temperature decreases, aggregation into larger structures commences, involving the C-7 propionate as a bridging group.

C. CHLOROPHYLL b

The dimeric structure of Chl **b** is much more complicated than that of Chl **a** due to the presence of an additional coordinating function in the molecule. Abraham and Smith,[82,83] using aggregation shifts obtained by Closs et al.,[13] examined the dimer structure of Chl **b**. As expected, unlike Chl **a**, there are two highly shielded regions in the aggregation map, one around the C-3 formyl group and one around the C-9 carbonyl group. Closs suggested that this is consistent with the presence of two sorts of dimers of comparable stability. Alternatively, in the case of trimers of dimers of comparable stability. Alternatively, in the case of trimers or higher aggregates, bonding could occur between the magnesium atom of different molecules and both the C-3 and C-9 carbonyls. Analysis of the shifts revealed that no symmetrical structure is capable of explaining the observed aggregation shifts; however, an unsymmetrical structure was proposed. (Figure 14 shows the proposed geometry for dimeric Chl **b**.) The displacement coordinates for this dimer being 1.5, 5.5, and 6.0 Å (x, y, and z). The interplane separation is very similar to that for Chl **a**, suggesting the presence of a hydrogen bonding network involving a water molecule. The calculated normalized aggregation shifts give good agreement for all the shifts except the C-3a formyl group. The formyl group is involved in bonding to the Mg via a water molecule and may rotate out of the plane in order to facilitate this bonding, inducing a large upfield shift for the formyl proton. The poor agreement obtained for the direct dimer calculation suggests that the observed shifts obtained by Closs et al. are due partly to aggregates larger than two. The structure proposed for Chl **b** allows interaction of the magnesium atoms with both the C-3 formyl group and the carbonyl groups of C-9 and C-10. Like the piggyback model proposed for Chl **a** and pyroChl **a**, the head-to-head structure of Chl **b** can form larger aggregates using precisely the same bonding as in the dimer itself. This is important since it allows higher aggregation to form relatively easily.

E. BACTERIOCHLOROPHYLLS

The aggregation behavior of BChl **a** has been observed by Katz et al.[93] and more recently by Brereton and Sanders.[76] Like Chl **b**, two highly shielded regions of the molecule were observed in the aggregation map.[7] Titration of a solution of BChl **a** in benzene with acetone gave a value for K_3 of 0.1 l/mol (10 m*M* concentration). The same titration, but with pyridine, gave a much steeper titration curve with a value of K_3 = 15 l/mol.[76] Abraham et al. have investigated the bifunctional dimer of methyl-BChlid **d**.[84] The complexation interaction in this molecule is sufficiently strong that the molecules in the aggregate are in the slow exchange limit and distinct spectra from the two molecules in the dimer are observed. This unique phenomenon shows immediately that the dimer cannot have C_2 symmetry, eliminating the Fong model as a possible dimer structure. Hence, only two possible dimeric structures, the face-to-face and piggyback models, were examined. (Table 14 shows the observed and calculated complexation shifts for BChlid **d**.) Both models gave reasonable

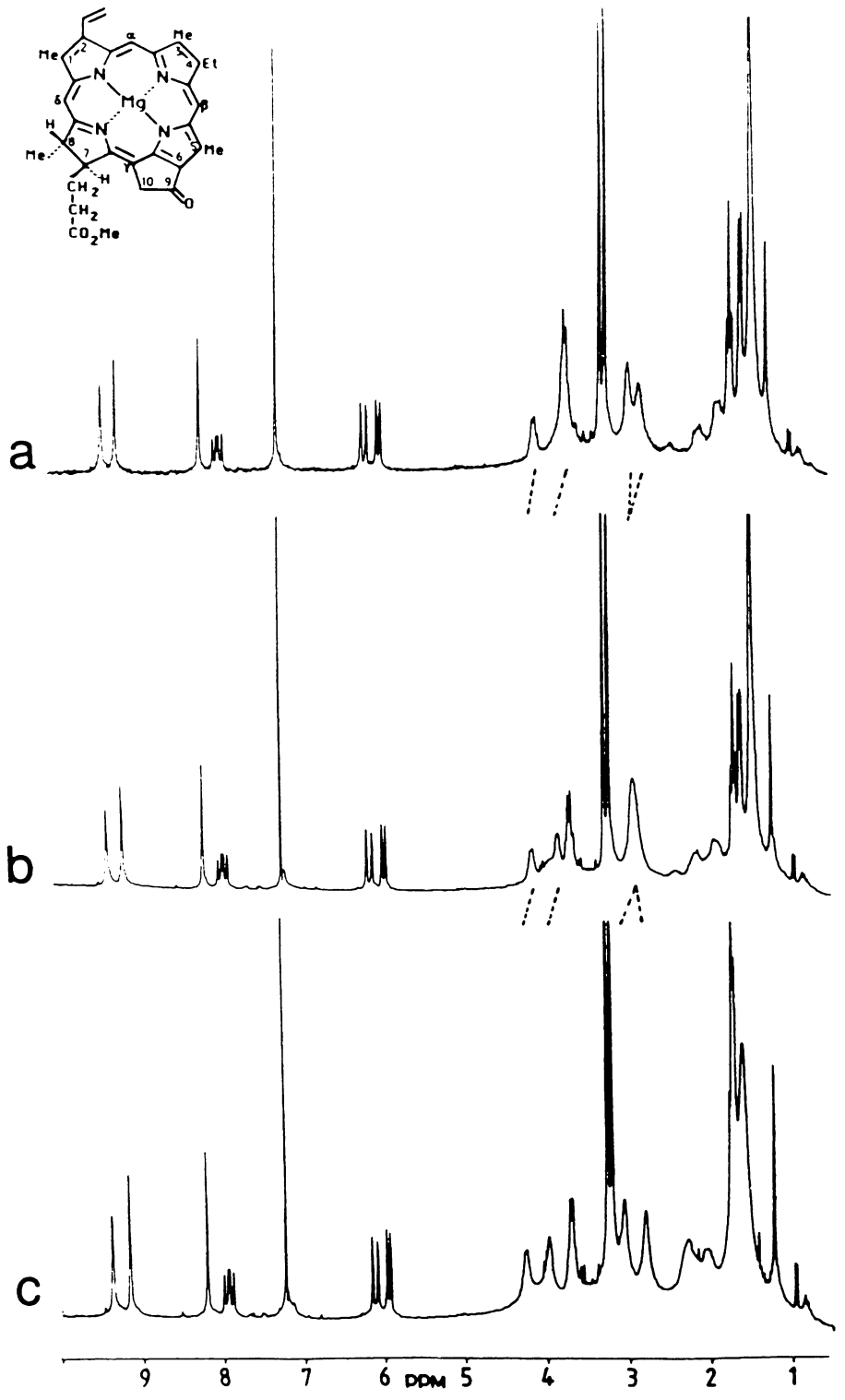

FIGURE 13. ^{1}H NMR spectra of methyl-pyro-Chlid **a** in $CDCl_3$ solution at (a) 299 K, (b) 279 K, and (c) 259 K. (From Abraham, R. J., Rowan, A. E., Goff, D. A., Mansfield, K. E., and Smith, K. M., *J. Chem. Soc. Perkin Trans. 2*, 1633, 1989. With permission.)

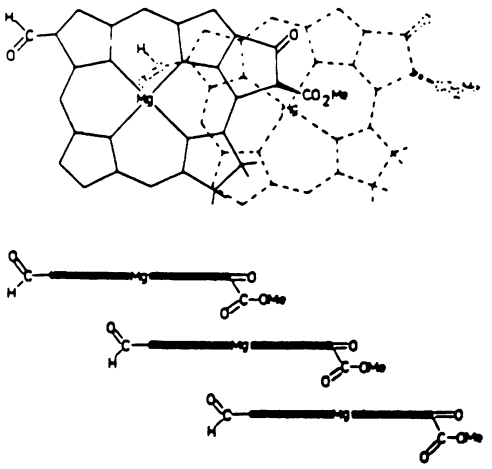

FIGURE 14. Proposed dimer geometry for Chl **b**. (Reprinted from Abraham, R. J. and Smith, K. M., *J. Am. Chem. Soc.*, 105, 5734, 1983. Copyright 1983, American Chemical Society.)

TABLE 14
Observed and Calculated Complexation Shifts[a] (Δδ) for Methyl-BChlid d [Et, Et] (1)

Proton	Obs. shifts	Calculated shifts	
		Piggyback	Face-to-face
Meso α	−2.82, −2.10	−2.73, −2.19	−2.76, −2.16
Meso β	0.05, 0.05	0.12, 0.12	0.18, 0.18
Meso δ	−0.02, −0.49	−0.03, −0.39	−0.14, −0.43
1-Me	−1.37, −2.10	−1.35, −2.26	−1.34, −2.17
3-Me	−0.12, 0.17	−0.31, −0.12	−0.14, 0.02
2b-Me	−1.62, −1.29	−1.70, −1.48	−1.85, −1.79
7d-OMe	−0.06, −0.62	0.09, −0.80	−0.04, −0.80
4a-CH_2	0.19, 0.09	0.19, 0.07	0.25, 0.23
4b-Me	−0.02, 0.84	−0.02, 0.30	0.03, 0.04
5a-CH_2	0.11, −0.03	0.12, 0.08	0.14, 0.13
5b-Me	0.03, 0.03	0.04, 0.15	0.05, 0.05
7-H	0.33, −0.07	0.18, 0.07	0.09, 0.08
8-H	0.12, 0.12	0.05, 0.27	0.36, 0.40
8-Me	0.25, −0.37	0.31, −0.04	0.00, −0.04
10-CH_2	0.22, −0.24	0.07, 0.14	0.17, 0.18
	0.09, −0.10	0.13, 0.07	0.09, 0.09

[a] $>\delta = \delta_{complex} - \delta_{monomer}$.

Reprinted from Abraham, R. J., Smith, K. M., Bobe, F. W., and Goff, D. A., *J. Am. Chem. Soc.*, 108, 1111, 1986. Copyright 1986, American Chemical Society.

agreement with the observed complexation shifts. The piggyback model, however, more easily rationalizes the complexation shifts of the side chain protons and, in particular, those of the C-7 propionate group. In the face-to-face model, both C-7 esters are either *endo* or *exo*, while in the piggyback model, one C-7 propionate experiences a complexation shift while the other is *exo* to the dimer and is unaffected. (Figure 15 shows the proposed dimer structures and the possible hydrogen bonding pathways.)

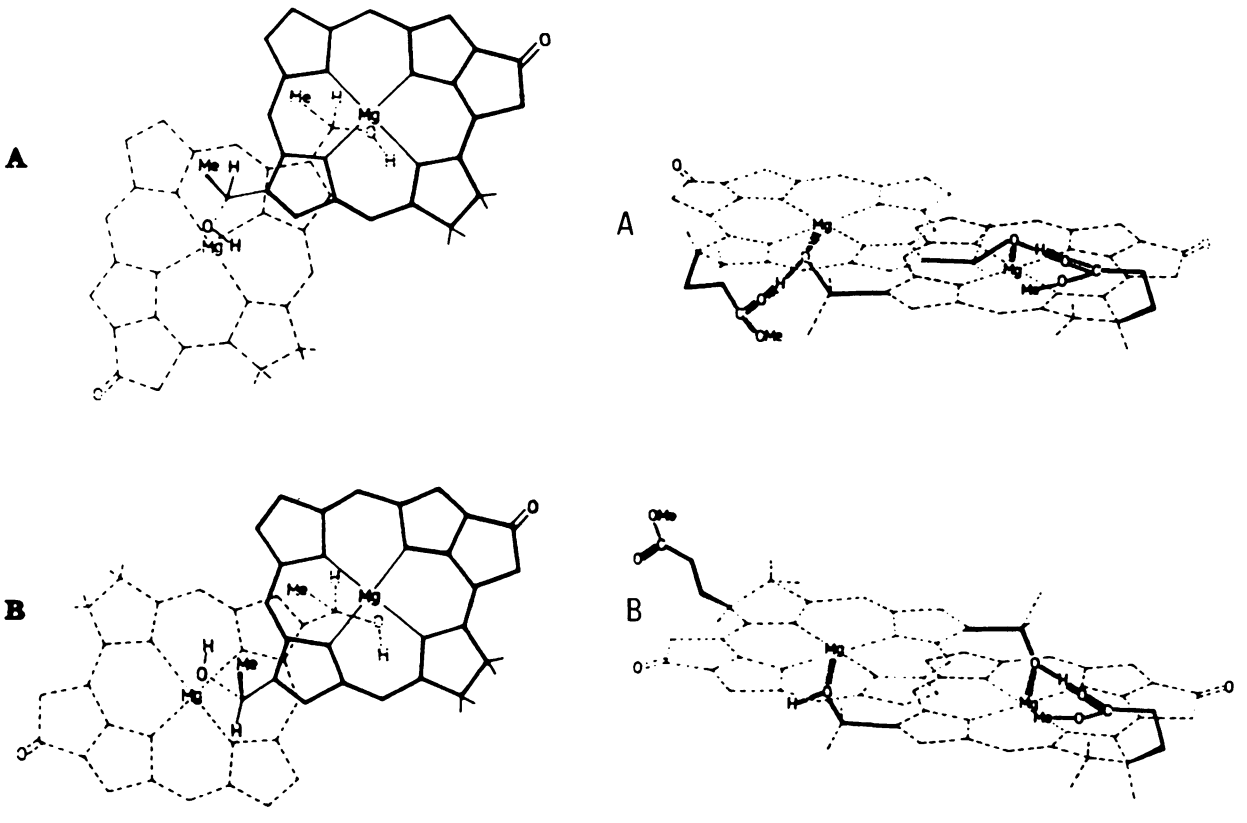

FIGURE 15. Proposed dimer geometry for Bchl **d** and the hydrogen bonding network. (A) Face-to-face model; (B) piggyback model. (Reprinted from Abraham, R. J., Smith, K. M., Bobe, F. W., and Goff, D. A., *J. Am. Chem. Soc.*, 108, 1111, 1986. Copyright 1986, American Chemical Society.)

The extremely stable dimer complex (estimated dissociation energy of 11 kcal/mol) and the presence of no oligomer in solution can be best accounted for by the piggyback model. The slow rate of interchange of the two molecules in the dimer is consistent with a dissociation mechanism with a large activation energy. In the piggyback model, the molecules cannot interchange without dissociating; however, in the face-to-face model, exchange between sites could occur without dissociation by simple lateral movement of the BChlid **d** molecules. Examination of the very similar BChl **c** species in chloroform shows effects similar to that seen for BChlid **d** and clearly forms a similar dimer.

F. SOLID-STATE NMR OF CHLOROPHYLL

There are good reasons to suppose that Chl *in vivo* is largely immobilized, unlike that observed in solution. New developments in NMR theory and instrumentation now make it possible to obtain useful high-resolution NMR spectra of immobilized (solid) samples. Brown et al.[94] have recorded the solid-state cross polarization/magic angle ^{13}C NMR spectra of Chl **a**-water aggregates, methyl-pyro-Chl **a**, and methyl-pyro-Pheid **a**. In the solid state, hydrated Chl **a** forms aggregates of stacked macrocycles with an outer layer of phytyl chains, much as in the case in nonnucleophilic organic solvents. Unfortunately, in this technique, the aggregation shifts are near the limits of resolution of the spectrum.

Examination of the Mg-free pheophorbide shows many changes in comparison to Chl **a**, especially in the aromatic region. However, little change is observed for the C-9 or C-7_c carbonyl carbons. Either the change in chemical shifts of the C-9 is very small upon forming a water bridge to the magnesium, or bridging by a water molecule is less important for ring stacking in the solid when the solvent effect of the phytyl is removed.

Using the same technique (^{13}C CP/MAS), Nozawa et al.[95] looked at the solid-state ^{13}C NMR spectra of the light-harvesting bacteriochlorophyll-protein complex 2 (LH2) of *Rp. palustris*. The resolved ^{13}C NMR peaks which can be assigned to BChl **a** are only those for the methyl carbon at 10 ppm and the phytyl methine carbons at 37.5 ppm. The olefinic carbons and the carbonyl carbons for BChl **a** are not resolved under large signals from proteins and lipids. The measured T_1 values for the methyl (8 to 10 ms) and the phytyl (6 to 8 ms) residues indicate that the phytol chain is buried in the protein rather than in the lipid fatty acid.

^1H NMR has been more revealing than ^{13}C NMR in investigating chlorophyll aggregation phenomena in solution. This may also be the case for *in vitro* studies now that improved experimental techniques are becoming available to study *in vitro* ^1H NMR. Dijkema et al.[96] recently observed, using modern pulse techniques, the 500-MHz ^1H NMR spectra of the oligomers and monomers of Chl **a**/**b**-P_2, the major light-harvesting chlorophyll a/b protein complex of photosystem II. The observed chlorophyll resonances for the monomer Chl **a**/**b**-P_2 subunit were found to be different from that for a solution of Chl **a** and Chl **b** *in vitro*. This protein monomer consists of four Chl **a**, three Chl **b**, and one to two lutein molecules per monomer subunit. In an ideal case with all Chl **a** molecules equivalent and all Chl **b** molecules equivalent, one would expect to see five lines, the α- and β-protons from Chl **a** and the α, β and aldehydic proton resonances for Chl **b**. The δ-proton resonance is submerged under the protein signals. The observed spectra, however, only contained resonances attributable to the Chl **b** molecule. Hence, the Chl **b** molecules in the monomer subunit are all magnetically equivalent, while those of Chl **a** are not, and thus these resonances are not seen. To account for the equivalence of the three Chl **b** molecules, a trimeric structure was proposed with C_3 symmetry (this trimer molecule was originally proposed by Shepansky and Knox[97]). With the aid of ring current calculations using the method developed by Abraham et al. (see above), the structure of the trimer was refined. However, the solution obtained was determined using only four shifts and consequently is underdetermined. The greater availability of high-field NMR facilities and the new improved pulse techniques will

in the future enable complete analysis of these biologically important protein-chlorophyll aggregate structures.

ACKNOWLEDGMENTS

This research was supported by the Scientific Affairs Division of NATO (RG0218/87) and the SERC (AER).

REFERENCES

1. **Clayton, R. K. and Sistrom, W. R., Eds.,** *The Photosynthetic Bacteria*, Plenum Press, New York, 1978.
2. **Govindjee, Ed.,** *Bioenergetics of Photosynthesis*, Academic Press, New York, 1975.
3. Chlorophyll organisation and energy transfer in photosynthesis, *Ciba Found. Symp.*, 61, 1979.
4. **Katz, J. J., Dougherty, R. C., and Boucher, L. J.,** *The Chlorophylls*, Vernon, L. P. and Seely, G. R., Eds., Academic Press, New York, 1966, 185.
5. **Scheer, H. and Katz, J. J.,** *Porphyrins and Metalloporphyrins*, Smith, K., Ed., Elsevier, Amsterdam, 1975, 399.
6. **Katz, J. J., Shipman, L. L., Cotton, T. M., and Janson, T. R.,** in *The Porphyrins*, Dolphin, D., Ed., Academic Press, New York, 1979, 1, 413.
7. **Katz, J. J. and Brown, C. G.,** Nuclear magnetic resonance spectroscopy of chlorophylls and corrins, *Bull. Magn. Reson.*, 5, 3, 1983.
8. **Abraham, R. J.,** The proton magnetic resonance spectra of porphyrins. II. Ring current effects in the porphyrins, *Mol. Phys.*, 4, 145, 1961.
9. **Becker, E. D. and Bradley, R. B.,** Effects of ring currents on the nmr spectra of porphyrins, *J. Chem. Phys.*, 31, 1413, 1959.
10. **Abraham, R. J., Smith, K. M., Goff, D. A., and Lai, J. J.,** Nmr spectra of porphyrins 18. A ring current model for chlorophyll derivatives, *J. Am. Chem. Soc.*, 104, 4332, 1982.
11. **Kooyman, R. P. H. and Schaafma, T. J.,** Nuclear spin relaxation and ring current shifts in chlorophyll dimers, *J. Am. Chem. Soc.*, 106, 551, 1984.
12. **Abraham, R. J., Goff, D. A., and Smith, K. M.,** Nmr spectra of porphyrins. XXXV. An examination of the proposed models of chlorophyll a dimer, *J. Chem. Soc. Perkin Trans. 1*, 2443, 1988.
13. **Closs, G. L., Katz, J. J., Pennington, F. C., Thomas, M. R., and Strain, H. H.,** Nuclear magnetic resonance spectra and molecular association of chlorophylls a and b, methyl chlorophyllides, pheophytins and methyl pheophorbides, *J. Am. Chem. Soc.*, 85, 3809, 1963.
14. **Smith, K. M., Goff, D. A., and Abraham, R. J.,** The nmr spectra of porphyrins 27. Proton nmr spectra of chlorophyll *a* and pheophytin *a*, *Org. Magn. Reson.*, 22, 779, 1984.
15. **Goff, D. A.,** Synthetic and Structural Studies of Bacterio Chlorophylls-D, Ph.D. thesis, University of California, Davis, 1984, 272.
16. **Goff, D. A.,** Synthetic and Structural Studies of Bacterio Chlorophylls-D, Ph.D. thesis, University of California, Davis, 1984, 36.
17. **Trowitzch, W.,** The assignment of the ^{1}H nmr signals to the methine bridge H-atoms in chlorophyll atoms, *Org. Magn. Reson.*, 8, 59, 1976.
18. **Brockmann, H., Trowitzsch, W., and Wray, V.,** The dilution behaviour of chlorophyll derivatives possessing α-hydroxyethyl groups, *Org. Magn. Reson.*, 8, 380, 1976.
19. **Smith, K. M., Goff, D. A., and Abraham, R. J.,** Proton magnetic study of the conformation of ring d and its side chains in chlorophyll derivatives, *Tetrahedron Lett.*, 22, 4873, 1981.
20. **Smith, K. M., Goff, D. A., and Abraham, R. J.,** Nmr spectra of porphyrins 29. Conformation of the propionic ester side chain in chlorophyll derivatives, *J. Org. Chem.*, 52, 176, 1987.
21. **Chow, H. C., Serlin, R., and Strouce, C. E.,** The crystal and molecular structure and absolute configuration of ethyl chlorophyllide a dihydrate. A model for the different spectral forms of chlorophyll *a*, *J. Am. Chem. Soc.*, 97, 7230, 1975.
22. **Fischer, M. S., Templeton, D. H., Zalkin, A., and Calvin, M.,** Crystal and molecular structure of methyl pheophorbide with applications to the chlorophyll arrangement in photosynthetic lamellae, *J. Am. Chem. Soc.*, 94, 3613, 1972.
23. **Goff, D. A.,** Synthetic and Structural Studies of Bacterio Chlorophylls-D, Ph.D. thesis, University of California, Davis, 1984, 163.

24. **Lötjönen, S., Michalski, T. J., Norris, J. R., and Hynninen, P. H.,** High field proton nmr study of the liquid solution structure of monomeric bacteriochlorophyll a and chlorophyll a, *Magn. Reson. Chem.*, 25, 670, 1987.
25. **Dougherty, R. C., Strain, H. H., Svec, W. A., Uphaus, R. A., and Katz, J. J.,** The structure properties and distribution of chlorophyll c, *J. Am. Chem. Soc.*, 92, 2826, 1970.
26. **Katz, J. J., Strain, H. H., Harkness, A. L., Studier, M. H., Svec, W. A., Janson, T. R., and Cope, B. T.,** Esterifying alcohols in the chlorophylls of purple photosynthetic bacteria. A new chlorophyll bacteriochlorophyll (gg), all *trans* geranyl geranyl bacteriochlorophyllide a, *J. Am. Chem. Soc.*, 94, 7938, 1972.
27. **Risch, N., Brockmann, H., Jr., Gloe, A., and Trowitzsch, W.,** Bacterio-Chlorophyll e, ein neues Chlorophyll aus braumen arten van Chlorobiaceae, *Justus Liebigs Ann. Chem.*, p. 566, 1976.
28. **Brockmann, H., Jr. and Lipinski, A.,** Bacteriochlorophyll g. A new bacteriochlorophyll from heliobacterium chlorum, *Arch. Microbiol.*, 136, 17, 1983.
29. **Brockmann, H., Jr. and Knobloch, G.,** Ein neues Bacteriochlorophyll aus *Rhodospirillium rubrum*, *Arch. Microbiol.*, 85, 123, 1972.
30. **Rapoport, H. and Harlow, H. P.,** Chlorobium chlorophyll 660. The esterifying alcohol, *Plant Cell Physiol.*, 4, 49, 1963.
31. **Holt, A. S., Hughes, D. W., Kende, H. J., and Purdie, J. W.,** Chlorophylls of green photosynthetic bacteria, *Plant Cell Physiol.*, 4, 49, 1963.
32. **Bothner-By, A. A., Castellano, S., Ebersole, S. J., and Gunther, H.,** The proton magnetic resonance spectra of olefins V. 3-Chloro- and 3-methoxypropenes, *J. Am. Chem. Soc.*, 88, 2466, 1966.
33. **Brereton, R. G. and Sanders, J. K. M.,** Coordination and aggregation of bacteriochlorophyll *a*. A nmr and electronic absorption study, *J. Chem. Soc. Perkin Trans. 1*, 423, 1983.
34. **Scheer, H., Svec, W. A., Cope, B. T., Studier, M. H., Scott, R. G., and Katz, J. J.,** The structure of bacteriochlorophyll b′, *J. Am. Chem. Soc.*, 96, 3714, 1974.
35. **Risch, N., Brockmann, H., Jr., and Gloe, A.,** Strukturaufklarung von neuartigen Bacteriochlorophyllen aus Chloroflexus aurantiacus, *Justus Liebigs Ann. Chem.*, p. 408, 1979.
36. **Goff, D. A.,** Synthetic and Structural Studies of Bacterio Chlorophylls-D, Ph.D. thesis, University of California, Davis, 1984, 97.
37. **Houghton, J. D., Jones, O. T. G., Quirke, J. M. E., Murray, M., and Honeyboume, C. L.,** 2-(1-Hydroxyethyl)-2-desvinyl chlorophyllide *a*. Characterisation by nOe, nmr of a novel pigment obtained from mutants of *Rhodopseudomonas sphaeroides*, *Tetrahedron Lett.*, 24, 5703, 1983.
38. **Sanders, J. K. M., Waterton, J. C., and Denniss, I. S.,** Spin-lattice relaxation, nuclear Overhauser enhancements and long range coupling in chlorophylls and metalloporphyrins, *J. Chem. Soc. Perkin Trans. 1*, 1150, 1978.
39. **Sanders, J. K. M.,** Nmr spectral changes as a probe of chlorophyll chemistry, *Chem. Soc. Rev.*, 6, 467, 1977.
40. **Pennington, F. C., Strain, H. H., Svec, W. A., and Katz, J. J.,** Preparation and properties of pyrochlorophyll *a*, methyl pyrochlorophyllide *a*, pyropheophytin *a* and methyl pyropheophorbides *a* derived from chlorophyll by decarbomethoxylation, *J. Am. Chem. Soc.*, 86, 1418, 1964.
41. **Hynninen, P. H.,** Keto-enol tautomerism of chlorophylls *a* and *b*. The nature of chlorophylls *a′* and *b′*, *Acta Chem. Scand.*, 27, 1487, 1973.
42. **Hynninen, P. H., Wasielewski, M. R., and Katz, J. J.,** Chlorophylls VI. Epimerisation and enolisation of chlorophyll *a* and its magnesium free derivatives, *Acta Chem. Scand. Ser. B*, 33, 637, 1979.
43. **Hynninen, P. H. and Lötjönen, S.,** Large scale preparation of crystalline 10(*S*)-chlorophylls *a* and *b*, *Synthesis*, p. 705, 1983.

43a. **Hynninen, P. H. and Lötjönen, S.,** An improved method for the preparation of 10(*R*)- and 10(*S*)-pheophytins *a* and *b*, *Synthesis*, p. 708, 1983.

44. **Hynninen, P. H. and Lötjönen, S.,** Steric interactions between the peripheral substituents of 10(*S*)-chlorophyll derivatives and its conformational consequences, a proton magnetic resonance study, *Magn. Reson. Chem.*, 23, 605, 1985.

44a. **Watanabe, T., Mozaki, H., and Nakazato, M.,** Chlorophyll a/a′ epiermization in organic solvents, *Biochim. Biophys. Acta*, 892, 197, 1987.

45. **Ellsworth, P. A. and Storm, C. B.,** Methyl-10-epipheophorbide a: an unusual epimeric stability relative to chlorophyll *a* or *a′*, *J. Org. Chem.*, 43, 281, 1978.
46. **Katz, J. J., Dougherty, R. C., Pennington, F. C., Strain, H. H., and Closs, G. L.,** Hydrogen exchange at methine and C-10 positions in chlorophyll, *J. Am. Chem. Soc.*, 85, 4049, 1963.
47. **Willslater, R. and Stoll, A.,** *Investigations of Chlorophyll* (transl.), Science Press, Lancaster, PA, 1928, 131.
48. **Franck, J., Rosenberg, J. L., and Weiss, C.,** *Luminence of Organic and Inorganic Materials*, Kallman, M. P. and Spruch, G. M., Eds., John Wiley & Sons, New York, 1962.

49. **Mauzerall, D. and Chivis, A.,** A novel cyclic approach to oxygen producing mechanism of photosynthesis, *J. Theor. Biol.*, 42, 387, 1973.
50. **Scheer, H. and Katz, J. J.,** New peripheral metal complexes related to chlorophyll, *J. Am. Chem. Soc.*, 97, 3273, 1975.
51. **Hynninen, P. H. and Sievers, G.,** Conformations of chlorophylls *a* and *a'* and their magnesium free derivatives as revealed by circular dichroism and proton magnetic resonance, *Z. Naturforsch. Teil B*, 36, 1000, 1981.
52. **Smith, K. M. and Unsworth, J. F.,** The nuclear magnetic resonance spectra of porphyrins 9. ^{13}C Nmr spectra of some chlorins and other chlorophyll degradation products, *Tetrahedron*, 31, 367, 1975.
53. **Janson, T. R. and Katz, J. J.,** Chlorophyll-chlorophyll interactions from ^{1}H and ^{13}C nmr spectroscopy, *Ann. N.Y. Acad. Sci.*, 206, 579, 1973.
54. **Brereton, R. G. and Sanders, J. K. M.,** Bacteriochlorophyll *a*. Influence of axial coordination of reactivity and stability. Design of an improved extraction procedure, *J. Chem. Soc. Perkin Trans. 1*, 423, 1983.

54a. **Schaber, P. M., Hunt, J. E., Fries, R., and Katz, J. J.,** High performance liquid chromatographic study of the chlorophyll allomerization reaction, *J. Chromatogr.*, 316, 25, 1984.

55. **Brereton, R. G., Rajananda, V., Blake, T. J., Sanders, J. K. M., and Williams, D. H.,** In beam electron impact mass spectroscopy, the structure of a bacteriochlorophyll allomer, *Tetrahedron Lett.*, 21, 1671, 1980.
56. **Lincoln, D. W., Wray, V., Brockmann, H., Jr., and Trowitzsch, W.,** ^{13}C nmr studies of porphyrins and related compounds of chlorophyll derivatives, *J. Chem. Soc. Perkin Trans. 2*, 1920, 1974.
57. **Smith, K. M. and Unsworth, J. F.,** The nmr spectra of porphyrins 9. ^{13}C nmr spectra of some chlorins and other chlorophyll degradation products, *Tetrahedron*, 31, 367, 1975.
58. **Lötjönen, S. and Hynninen, P. H.,** Complete assignment of the ^{13}C nmr spectrum of chlorophyll *a*, *Org. Magn. Reson.*, 16, 304, 1981.
59. **Lötjönen, S. and Hynninen, P. H.,** ^{13}C nmr spectra of chlorophyll *a*, chlorophyll *a'*, pyrochlorophyll *a* and the corresponding pheophytins, *Org. Magn. Reson.*, 21, 757, 1983.
60. **Boxer, S. G., Gloss, G. L., and Katz, J. J.,** The effect of magnesium coordination on the ^{13}C and ^{15}N magnetic resonance spectra of chlorophyll *a*. The relative energies of nitrogen $n\pi^*$ states as deduced from a complete assignment of chemical shifts, *J. Am. Chem. Soc.*, 96, 7058, 1974.
61. **Katz, J. J., Shipman, L. L., Cotton, T. M., and Jansen, T. R.,** in *The Porphyrins*, Dolphin, D., Ed., Academic Press, New York, 1979, 1, 413.
62. **Strouse, C. E., Koolman, V. H., and Matwiyoff, N. A.,** ^{13}C nmr spectra of ^{13}C enriched chlorophylls *a* and *b*, *Biochem. Biophys. Res. Commun.*, 46, 328, 1972.
63. **Matwiyoff, N. A. and Burnham, B. F.,** ^{13}C nmr spectroscopy of tetrapyroles, *Ann. N.Y. Acad. Sci.*, 206, 365, 1973.
64. **Goodman, P. A., Oldfield, E., and Allerhand, A.,** Assignment in the natural abundance ^{13}C nmr spectrum of chlorophyll *a* and a study of segmental motion in neat phytol, *J. Am. Chem. Soc.*, 95, 7553, 1973.
65. **Wray, V., Jürgens, U., and Brockmann, H., Jr.,** Electrophilic reactions of chlorin derivatives and a comprehensive collection of ^{13}C data of these products and closely related compounds, *Tetrahedron*, 35, 2275, 1979.
66. **Smith, K. M., Bushell, M. J., Rimmer, J., and Unsworth, J. F.,** Bacteriochlorophylls *c* from chloropseudomonas ethylicium composition and nmr studies of the pheophorbides and derivatives, *J. Am. Chem. Soc.*, 102, 2437, 1980.
67. **Spangler, D., Maggiora, G. M., Shipman, L. L., and Christoffersen, J.,** Stereoelectronic properties of photosynthetic and related systems. *Ab initio* quantum mechanical ground state characterisation of magnesium phorphine, magnesium chlorin and ethyl chlorophyllide *a*, *J. Am. Chem. Soc.*, 99, 7478, 1977.
68. **Risch, N. and Brockmann, H., Jr.,** Chlorophyll *b*. Totalzuarding des ^{13}C nmr Spektrums, *Tetrahedron Lett.*, 24, 173, 1983.
69. **Lötjönen, S. and Hynninen, P. H.,** ^{13}C nmr spectroscopic evidence for the existence of the monocation of pyropheophytin *a*, *Org. Magn. Reson.*, 22, 511, 1984.
70. **Abraham, R. J., Hawkes, G. E., and Smith, K. M.,** The nmr spectra of porphyrins. VIII. The ^{13}C nmr spectra of some porphyrins and metalloporphyrins, *J. Chem. Soc. Perkin Trans. 2*, 627, 1974.
71. **Abraham, R. J., Hawkes, G. E., Hudson, M. F., and Smith, K. M.,** The nmr spectra of porphyrins. X. ^{13}C nmr spectra of some meso tetraporphyrins and their metal chelates, *J. Chem. Soc. Perkin Trans. 2*, 204, 1975.
72. **Brereton, R. G. and Sanders, J. K. M.,** Bacteriochlorophyll *a* assignment of the natural abundance ^{13}C nmr spectrum. Use of power spectra, *J. Chem. Soc. Perkin Trans. 1*, 435, 1983.
73. **Brereton, R. G. and Sibisi, S. P.,** Absolute value and phased Fourier transform nmr spectra. Shift distortions and resolution, *J. Magn. Reson.*, 48, 447, 1982.
74. **Oh-hama, T., Seto, H., and Miyachi, S.,** ^{13}C nmr studies on bacterio-chlorophyll *a*, biosynthesis on *Rhodopseudomonas spheroides* S, *Arch. Biochem. Biophys.*, 72, 237, 1985.
75. **Dougherty, R. C., Norman, G. D., and Katz, J. J.,** Deuteron-magnetic resonance, spectroscopy of large molecules, spectrum of chlorophyll *a*-d_{72}, *J. Am. Chem. Soc.*, 87, 5801, 1965.

76. **Brereton, R. G. and Sanders, J. K. M.,** Coordination and aggregation of bacteriochlorophyll *a*. An nmr and electronic study, *J. Chem. Soc. Perkin Trans. 1*, 423, 1983.
77. **Abraham, R. J., Goff, D. A., and Smith, K. M.,** Nmr spectra of porphyrins. XXXV. An examination of the proposed models of chlorophyll *a* dimer, *J. Chem. Soc. Perkin Trans. 1*, 2443, 1988.
78. **Waterton, R. J. and Sanders, J. K. M.,** Hyperfine coupling in chlorophyll radical cations. A nmr approach, *J. Am. Chem. Soc.*, 100, 4044, 1978.
79. **Fyfe, C. A.,** *Solid State Nmr for Chemists*, CFC Press, Guelph, 1983.
80. **Ballschmiter, K., Truesdell, K., and Katz, J. J.,** Aggregation of chlorophyll in non-polar solvents from molecular weight measurements, *Biochim. Biophys. Acta*, 184, 604, 1969.
81. **Abraham, R. J., Smith, K. M., Goff, D. A., and Lai, J. J.,** Nmr spectra of porphyrins. XVIII. A ring current model for chlorophyll derivatives, *J. Chem. Soc.*, 104, 4332, 1982.
82. **Abraham, R. J. and Smith, K. M.,** Nmr spectra of porphyrins. XXI. Applications of the ring current model to porphyrin and chlorophyll aggregation, *J. Am. Chem. Soc.*, 105, 5734, 1983.
83. **Abraham, R. J. and Smith, K. M.,** Novel proton nmr characterised structures for chlorophyll *a* and *b* aggregation in solution, *Tetrahedron Lett.*, 24, 2681, 1983.
84. **Abraham, R. J., Smith, K. M., Bobe, F. W., and Goff, D. A.,** Nmr spectra of porphyrins 28. Detailed solution structure of a bacteriochlorophyllide *d* dimer, *J. Am. Chem. Soc.*, 108, 1111, 1986.
85. **Shipman, L. L., Cotton, T. M., Norms, J. R., and Katz, J. J.,** New proposed model for structure of special pair chlorophyll, *Proc. Natl. Acad. Sci. U.S.A.*, 73, 1791, 1976.
86. **Houssier, C. and Seiver, K.,** Circular dichroism and magnetic circular dichroism of the chlorophyll and protochlorophyll pigments, *J. Am. Chem. Soc.*, 92, 779, 1970.
87. **Katz, J. J., Norris, J. R., and Shipman, L. L.,** Chlorophyll-proteins reaction centers and photosynthetic membranes, *Brookhaven Symp. Biol.*, 1976, 15.
88. **Kooyman, R. P. H. and Schaafsma, T. J.,** Nuclear spin-relaxation and ring current shifts in chlorophyll dimers, *J. Am. Chem. Soc.*, 106, 551, 1984.
89. **Fong, F. K. and Koester, V. J.,** Bonding interactions in anhydrous and hydrated chlorophyll *a*, *J. Am. Chem. Soc.*, 97, 6888, 1975.
90. **Abraham, R. J., Rowan, A. E., Goff, D. A., Mansfield, K. E., and Smith, K. M.,** Nmr spectra of porphyrins. XXXVII. The structure of the methyl pyrochlorophyllide *a* dimer, *J. Chem. Soc. Perkin Trans. 2*, 1633, 1989.
91. **Miller, J. R. and Dorough, G. D.,** Pyridinate complexes of some metallo derivatives of tetraphenylporphine and tetraphenylchlorin, *J. Am. Chem. Soc.*, 74, 3977, 1952.
92. **Kratky, C., Isenring, H. P., and Dunitz, J. D.,** Methylpyrochlorophyllide *a* monohydrate monoetherate, *Acta Crystallogr. Sect. B*, B33, 547, 1977.
93. **Wasielewski, M. R., Studier, M. H., and Katz, J. J.,** Covalently linked chlorophyll *a* dimer. A biomimetic model of special pair chlorophyll, *Proc. Natl. Acad. Sci. U.S.A.*, 73, 4282, 1976.
94. **Brown, C. E. Spencer, R. B., Burger, V. T., and Katz, J. J.,** Cross polarisation/magic angle sample spinning, ^{13}C nmr spectroscopic study of chlorophyll *a* in the solid state, *Proc. Natl. Acad. Sci. U.S.A.*, 81, 641, 1984.
95. **Nozawa, T., Nishimura, M., Hatano, M., Hayashi, H., and Shimada, K.,** High-resolution cross polarization/magic angle spinning ^{13}C nmr of intracytoplasmic membrane and light-harvesting bacteriochlorophyll-protein of photosynthetic bacteria, *Biochemistry*, 24, 1890, 1985.
96. **Dijkema, C., Searle, G. F. W., and Schaafsma, T. J.,** 500 MHz ^{1}H nmr of chlorophylls in the major light-harvesting chlorophyll-protein complex of photosystem II, *Biochem. Biophys. Res. Commun.*, 157, 1085, 1988.
97. **Shepanski, J. F. and Knox, R. S.,** Circular dichroism and optical properties of antenna chlorophyll proteins from higher plants, *Isr. J. Chem.*, 21, 325, 1981.